Investigation of Respiration Induced Strain Caused on the Rib

Undergraduate Honors Thesis

Presented in Partial Fulfillment of the Requirements for

Graduation with Distinction

at The Ohio State University

By

David J. Cagle

The Ohio State University

2011

Defense Committee:

Professor John Bolte, Adviser

Instructor Amanda Agnew

Approved by

Advisor

Undergraduate Program in Mechanical Engineering

ABSTRACT

Thoracic injuries specifically account for approximately 30% of serious injuries within the United States. Age-associated bone loss and a deterioration of bone quality in elderly patients' increases the likelihood of bone fractures during a thoracic impact. Bone quality can be quantified by examining microfeatures of bone, such as microfractures. Cyclic loading of ribs during normal respiration may contribute to the creation of fatigue damage in the form of microfractures, which can adversely affect bone strength. In order to observe the microdamage induced during a thoracic impact, which could lead to failure, the 'normal' condition of elderly ribs must be investigated prior to any manipulation. Since microfractures are initiated in regions of bone that experience high local strains, it is necessary to measure strain patterns in ribs during normal conditions of breathing. This will allow researchers to hypothesize possible locations of high microfracture density and identify those locations which may have an increased risk for failure. The objective of this study is to determine areas of high strain in the bony thorax during breathing. A Post-Mortem Human Subject was instrumented with 30 strain gauges to the cutaneous surface of ribs 2, 4,6,7,8 and 10 at anterior, middle (lateral), and posterior locations. A respirator bag was used to simulate shallow and deep respiratory patterns. The results showed that there was: 1) Significant difference between matching bilateral strain values during simulated respiration, 2) The strain values in the posterior region were statistically less than in the anterior region during simulated respiration but not significant, and 3) Strain values did not significantly vary by rib level during simulated respiration.

ACKNOWLEDGMENTS

I would like to thank my advisor, Professor John Bolte, for giving me the opportunity for this tremendous learning opportunity through my undergraduate research project and the assistance he has provided along this endeavor. I would especially like to thank Ph.D. student Amanda M. Agnew who helped me with extensive test preparation, experimentation, and overall support throughout the duration of my project. I would also like to thank the rest of The Ohio State University Injury Biomechanics Research Laboratory for their extensive efforts in experimental setup and experimentation. These individuals include: Julie Bing, Kyle Icke, Yun Seok Kang, Matthew Long, Brian Suntay, and Tony Vergis. Finally, I would like to thank the Injury Biomechanics Research Laboratory for allowing me to use their test facility equipment and financial support. Finally I'd like to thank Alex Kiturkes, University of Michigan, for his efforts on the final review of the thesis.

Table of Contents

Table of Figures

List of Tables

Introduction

Osteoporosis is often defined by a bone fracture caused by the loss of bone mass (Burr 1997). Reduction of bone mass is thought to contribute to an increased fracture rate, but it is not the only factor that will predispose an individual to a nontraumatic fracture. Thoracic injuries account for approximately 30% of serious injuries within the United States of America (Vezin 2009). Age-associated bone loss and a deterioration of bone quality in elderly patients' increases the likelihood of bone fractures during a thoracic impact (Hoshaw 1997). Microdamage accumulation reduces fracture toughness in tension significantly and may decrease fracture resistance (Burr 2003). Structurally, the trabecular matrix connectivity is reduced with a decrease in bone mass. Furthermore, fragility of the bone can be related directly to the cortical bone structure, which can be dependent on the tissue matrix mineralization or the accumulation of microdamage (Burr 2003). This microdamage can result from small loads that are applied repeatedly to the bone, having a direct effect on the bone quality.

In order to observe the microdamage induced during a thoracic impact, which could lead to failure, the 'normal' condition of elderly ribs must be investigated prior to any manipulation. Bone quality can be quantified by examining microfeatures of bone, such as microfractures. Cyclic loading of ribs during normal respiration may contribute to the creation of fatigue damage in the form of microfractures, which can adversely affect bone strength. Since microfractures are initiated in regions of bone which experience high local strains, it is necessary to measure strain patterns in ribs during normal conditions of breathing. "Understanding the detailed stress and strain redistribution process before fracture and its dependence on bone microstructure and geometry holds a key to the understanding of bone strength" (Ebacher 2007, 1265). This will

allow researchers to hypothesize possible locations of high microfracture density and identify those locations which may have an increased risk for failure.

In order to analyze the bony thorax for higher areas of strain, the mechanics of respiration should be understood for hypothesizing the maximum strain locations. The movement of the thoracic cage is coupled with the expansion and collapse of the diaphragm. The vertical movement of the thorax results from the combined extension and flexion of the vertebral column, resulting in an increased movement in the anterior parts of the chest than posterior parts (Wade 1953). "The thoracic cage is a large and massive structure and the redistribution of visceral weight that occurs with change of posture makes little difference either to its circumference or to the pattern of its movement. The smallness of the movements of chest expansion during rapid forced respiration may be related to the mass and inertia of the thoracic cage. Movements of chest expansion differ from diaphragmatic movements in that they can to some extent be inhibited voluntarily, at any rate in trained subjects" (Wade 1953, 210). The variable movement of the diaphragm can be somewhat controlled with the use of a Post Mortem Human Subject (PMHS). The movement of the PMHS thorax during respiration can be correlated to the movement of an *in vivo* subject through the use of a strain gauge band that can assess a change in the thoracic circumference (Russell 1994). The *in vivo* subject test was used to gather a baseline breathing strain pattern for the thorax. This pattern was used to validate the methods used in the PMHS methods section.

The objective of this study is to determine areas of high strain in the bony thorax during breathing. The experimental analysis will concentrate on three specific hypotheses: 1) There is no significant difference between matching bilateral strain values during simulated respiration, 2) Strain values in the posterior region will be significantly greater than in the anterior region

during simulated respiration, and 3) Strain values will significantly vary by rib level during simulated respiration.

The anatomical differences between the right and left sides of the thorax are presumed not to have a significant impact on strain caused by respiration. The left lung is smaller (two lobes) than the right lung (three lobes) (Clemente 1985). This is thought not to be a factor because it is assumed that the expansion of both lungs is similar, generating an equivalent pressure upon the bony thorax during inhalation. These justifications support the proposed hypothesis that there will be no significant difference in the matching bilateral strains.

The hypothesis that the posterior will experience greater strain than the anterior is based on a simplified model of the rib. Modeling the rib as a fixed beam, where the union between the rib and the spine represents the fixed support, and then adding and unknown loading function to the rib will cause strain at the posterior region of the rib. The unknown load function will create a resultant load that will cause a moment on the rib. This moment will create a higher deformation of the rib at the fixed location, thus causing an increase in strain. This rib and spine have been modeled as a simple fixed beam structure, Figure 1.

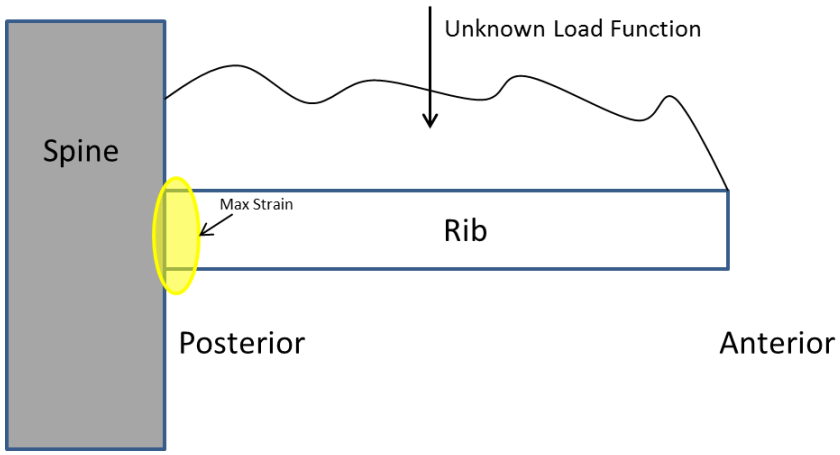

Figure 1: Simply supported beam model used to justify the hypothesis of greater strain caused by respiration posteriorly than anteriorly

The strain caused by respiration is thought to vary significantly in the superior and inferior directions due to the anatomical characteristics of the bony thorax. The ribs all connect slightly different to the sternum via cartilage. Ribs one thru seven connect directly to the sternum, while ribs eight and nine connect to cartilage of the seventh rib as does the tenth rib sometimes, though it can vary between subjects (Clemente 1985). Ribs eleven and twelve float and are not directly connected to the sternum (Clemente 1985). Ribs 7-10 share a connection to the sternum through connected costal cartilage, it is expected that the respiration induced strain will vary in the superior and inferior directions. This shared costal cartilage connection is expected to have a significant impact on the strain seen on these ribs. The skeletal structure of the thorax with different cartilage connections can be seen in Figure 2. A more in-depth anatomical description of the thorax and respiration will be highlighted in the next section.

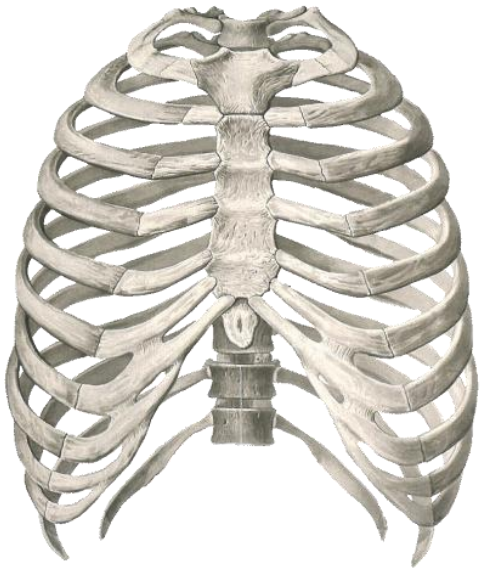

Figure 2: Bony skeletal thorax with cartilage connections to the sternum shown

Anatomy of the thorax and respiration

A firm understanding of the anatomy and the processes involved for respiration need to be firmly understood for the procedures, methods, discussion, and the proposed hypotheses. The following descriptions have been summarized from "Human Anatomy and Physiology" by Elaine N. Marieb to provide a thorough understanding of the bony thorax and respiration anatomy (Marieb 1998).

The bony thorax is composed of multiple elements; the thoracic vertebrae, ribs, costal cartilage and the sternum. The bony thorax serves as a protective structure for many of the body's vital organs, such as the heart and lungs. Furthermore, the thorax serves as a support structure for the upper limbs and provides attachment points for many muscles, particularly for the shoulders, chest, and back. The spaces in-between the ribs (intercostal spaces) play an important role during respiration. These muscles lift the thoracic cage as respiration occurs.

The connections with the intercostal cartilage between the ribs and the sternum have been hypothesized to have an important impact on strain caused by respiration. Therefore, it is important to understand the connections between the ribs and the sternum. The ribcage is composed of twelve pairs of ribs. As previously mentioned, ribs 1-7 attach directly to the sternum via costal cartilage and these ribs are known as 'true' ribs and hence ribs 8-10 are known as 'false' ribs because they do not connect directly to the sternum. Ribs 8-10 connect through the costal cartilage of rib seven. The 'floating' ribs (11 and 12) do not connect directly to the sternum, but instead are integrated into lateral body muscle wall. These ribs were not instrumented because of this anatomical difference. As with all ribs, they would experience a significantly altered loading pattern in an *in vivo* subject due to muscle activation as compared to a PMHS. Since the floating ribs are not attached via the sternum, their loading is reliant on muscle activation. This feature leads to their exclusion from instrumentation and investigation in this study. The importance of muscle activation in respiration directly affects the bony thorax and thus the expected strain caused by respiration on the thoracic cage.

The three main muscles involved in respiration are the internal and external intercostal muscles and the diaphragm. The internal and external intercostal muscles are arranged in-between the ribs and serve to aid opposing actions, inhalation (external) and exhalation (internal). The diaphragm serves as the primary muscle for inhalation activation. The contraction of the diaphragm increases the volume of the thorax. This act creates the pressure differential necessary to pull air into the lungs. The contraction of the diaphragm is also dependent on the muscular contractions of the abdomen to provide a firm fixed base as the thoracic cage moves.

The skeletal relations and connections of the bony thorax are equally important to the internal organs and orientation of these organs in the thoracic cage. The difference in lung size from right to left can be directly related to the location of the heart. The heart is on the left side of the thorax and occupies space. Therefore, the left lung is smaller than the right lung, having only two lobes as the right lung has three lobes.

Methods

For this study, both a live volunteer and a Post Mortem Human Subject were used. The following methods section will be broken down into *in vivo* testing, Post-Mortem Human Subject (PMHS) testing, and a data analysis section.

In vivo testing

The *in vivo* testing consisted of using an adult male subject. The male subject was 26 years of age, 70 inches tall, and weighed 175 lbs. To obtain the movement of the thorax, a chest band consisting of strain gauges spaced every inch around the band was used.

Figure 3: Chestband laid flat on ground; gauges every inch

This chest band was then attached to a Yokogawa data acquisition system (DAS), where the band was balanced. The balancing of the chest band consisted of obtaining a data trial where the chest band would be at steady state and experiencing no circumferential strains. This was

performed by laying the band flat on the ground and then applying an aluminum beam on top of it causing the band to be completely flat. Data was then collected from the band to obtain the steady state values of each of the strain gauges. The averages for each of the individual 40 strain gauges were used to subtract off the baseline strain for each strain gauge. After this procedure was performed, the band was wrapped around the *in vivo* subject's thorax. The band was hand tightened on the subject without causing severe discomfort. To ensure sufficient contact with the skin, double sided tape was applied directly to the subject and the underside of the chest band. The band was wrapped around the subject, leveling the chest band at the sternum. The location of the chest band gauges relative to the spine and sternum were recorded for the *in vivo subject* (Appendix A).

The data acquisition system was set at 100 Hz for 60 seconds, capturing data from all 40 strain gauge channels. The data was collected in units of strain (rad/mm). During the minute long test period, the subject was instructed to follow a specific breathing pattern which consisted of several steps. . The first procedural step required the subject to completely exhale and hold their breath for approximately ten seconds. This step was included to gain steady state values for the chest band strain gauges after it had been applied to the subject. After the initial ten seconds, the subject was then instructed to begin breathing normally for approximately 20 seconds, taking breaths as needed. Following the normal breathing section, the subject was instructed to breathe as deeply as possible three consecutive times, inhaling and then exhaling as completely as possible. After the deep breaths, the subject was instructed to again breathe normally for the duration of the test. This breathing sequence was repeated five times, collecting data for each test sequence.

Post-Mortem Human Subject Testing

The PMHS used in this study was male, 88 years of age, 71.25 inches, and weighed 205 lbs. The following section will outline the procedures used for the preparation of the PMHS subject along with the procedures used for testing the rib strain caused by respiration.

For the PMHS subject, both a bone mineral density (BMD) and a computed axial tomography (CAT) scan were performed prior to any manipulation. These tests were used to check for abnormalities or potential detrimental defects to testing results. The CAT scan revealed a minor scoliosis, Figure 4. Anthropometric data for the subject was also collected at this time (Appendix B). The scans revealed the presence of a pacemaker, one prosthetic knee, and two prosthetic hips. The pacemaker was removed from the subject prior to instrumentation, Figure 5.

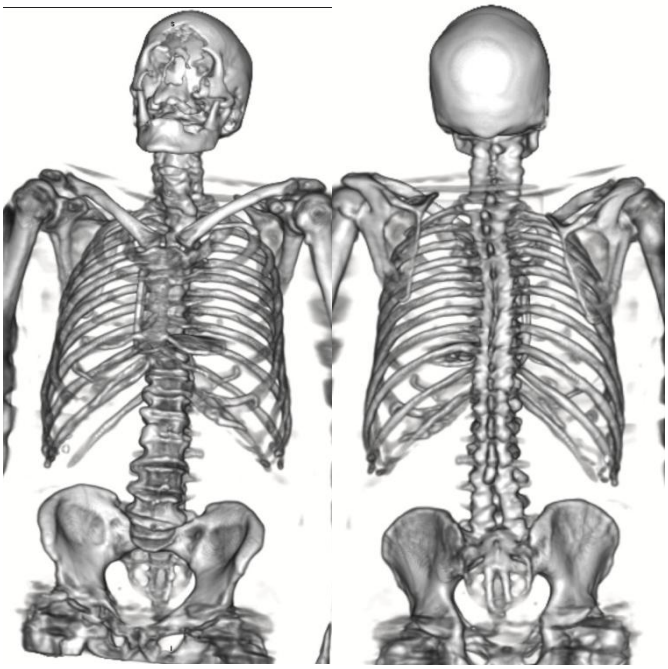

(a) (b)

Figure 4: (a) Reconstructed 3-D model of PMHS, anterior view of bony thorax (b) Posterior view, with slight scoliosis visible

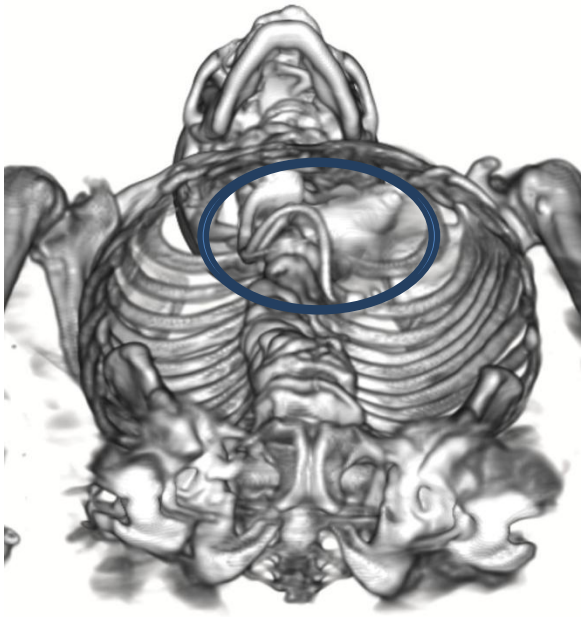

Figure 5: Inferior to superior view of the internal bony thorax; abnormality represents the pacemaker that was removed (highlighted with blue circle)

Both of the PMHS subject's upper limbs were removed from the thorax, including the scapula. The limbs were removed from the PMHS to gain access to the upper posterior rib locations for instrumentation. This procedure was performed by cutting all the necessary muscle, ligaments, and tendon attachments at the shoulder and cutting the clavicle mid-shaft. Special care was taken to keep the muscles of respiration (e.g. intercostals) and other thoracic muscles (e.g. latissimus dorsi intact), preserving the integrity of the thorax and respiration muscular system. The exclusion of muscular contractions experienced during respiration will undoubtedly reduce the expected strain on the bony thorax but will allow for a more unbiased replication of respiration.

The Post-Mortem Human Subject was instrumented with 30 strain gauges to the cutaneous surface of ribs 2, 4,6,7,8 and 10 at anterior, middle (lateral), and posterior locations. Prior experimentation describes that spatial attenuation of the strain gauge signal dictates the use of as many as five to six gauges per rib to properly map for fracture timing of the entire rib cage. The act of installing more than 100 strain gauges per PMHS chest is an invasive procedure and extremely costly in terms of time, instrumentation, and data acquisition channels (Gabrielli 2009). The goal of this experiment is to find the rough anatomical location of higher strain on the bony thorax, not a precision map of rib fracture. Therefore, a maximum of three gauges were used on any singular rib and not all ribs were instrumented. Due to confined number of data acquisition channels, not all ribs were instrumented anterior, middle and lateral.

In deep respiration, vertical movements of the thoracic cage occur. The extent is variable between individuals and is mostly marked at the end of deep inspiration and is always greater when subjects are erect than when in the supine position. Despite the great differences in the vertical movement of the thoracic cage in the erect and supine postures, the measurements of the total excursion of the diaphragm relative to the thoracic cage in these two postures are very similar (Wade 1953). To replicate the movement of the bony thorax, a respirator bag was used to simulate shallow and deep respiratory patterns on an erect PMHS. Pressurization of the lungs was determined to not supersede 10kPa, or approximately 102 cm H_2O, throughout the course of the experiment (Forman 2006). The cyclic pressurization and release of air was used to simulate the respiration experienced by *in vivo* subjects. The modeled respiration was used to create strain across the rib cage for analysis.

For testing, VISHAY general purpose strain gauges SR-4 were used (Figure 6). All strain gauges were tested with a voltmeter to ensure proper working status prior to installation.

The strain gauges were strengthened with electrical tape around the copper leads of the gauge to avoid failure during installation.

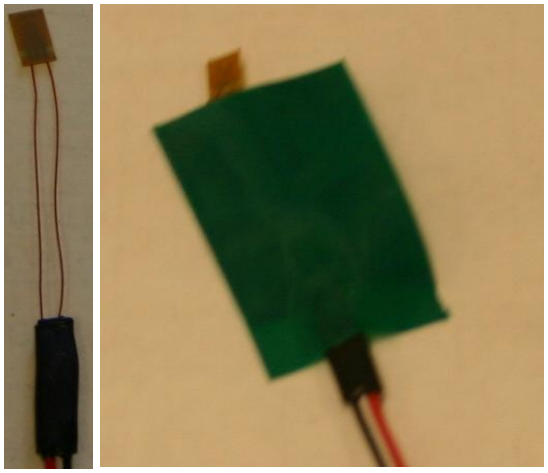

(a) (b)

Figure 6: (a) VISHAY general purpose strain gauge

(b) Leads strengthened with electrical tape

Catalyst was applied to the strain gauge to help the gauges adhere to the rib surface. All gauges were labeled by side (right-R, left-L), rib number, and location (anterior-A, middle-M, posterior-P). For example, label L8M refers to a strain gauge location on the left side, the number eight rib, at the middle location. Locations of applied gauges can be seen in Figure 7.

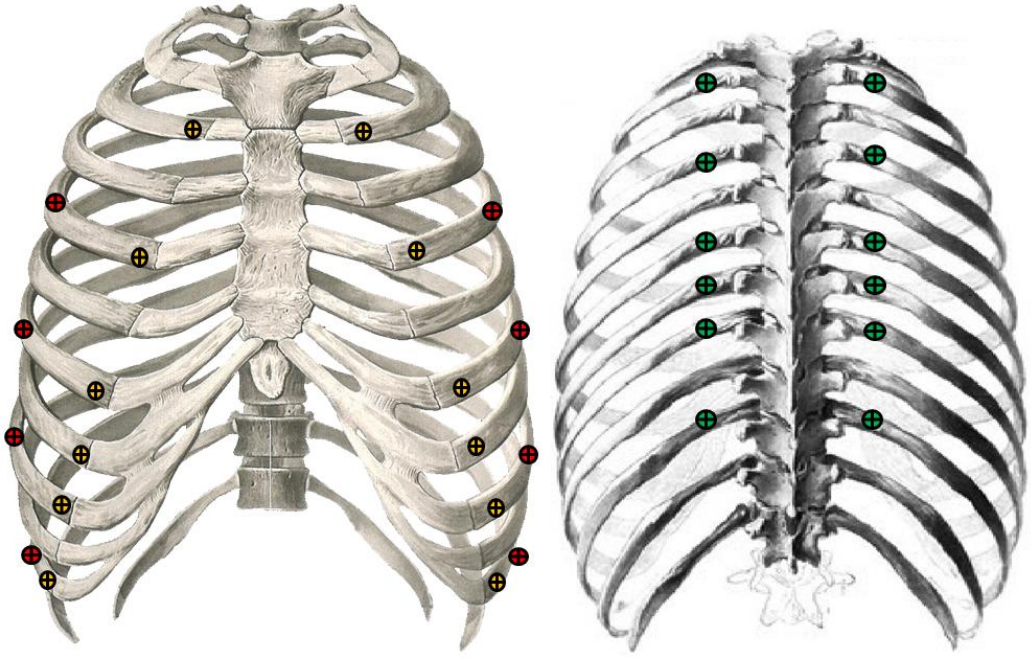

(a) (b)

Figure 7: Strain gauge locations (a) anterior view (b) posterior view

Ribs 2, 4, 6, 7, 8 and 10 were exposed by creating incisions along the rib body. The ribs were then scraped clean at the appropriate locations. An exposed rib that has been scraped to the bone surface prior to application of the strain gauge is shown in Figure 8.

Prior to gluing the strain gauge to the rib surface, the application site was swabbed with ether. The strain gauges were then glued to the rib and held in place for three minutes to ensure proper fixation. Installation of a strain gauge can be seen in Figure 9.

Measurements were taken to record the locations of the medial and anterior strain gauges (Appendix B). Posterior strain gauges were consistently applied at the costal angle. An example of a properly installed strain gauge can be seen in Figure 10. All gauges were again tested with a voltmeter to ensure proper working status. All defective strain gauges were removed and new

ones were applied as needed. After all of the anterior and medial strain gauges were applied and in correct working order, the incisions were sutured closed (Figure 11).

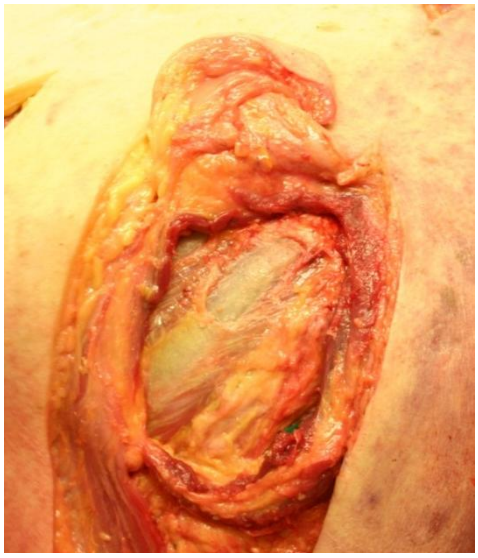

Figure 8: Exposed rib with cleaned bone surface

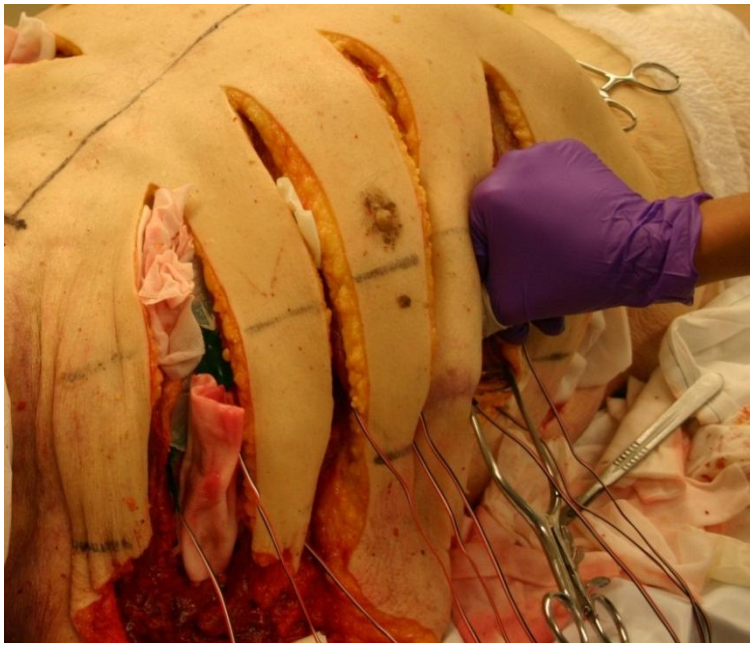

Figure 9: Application of the strain gauge to the rib

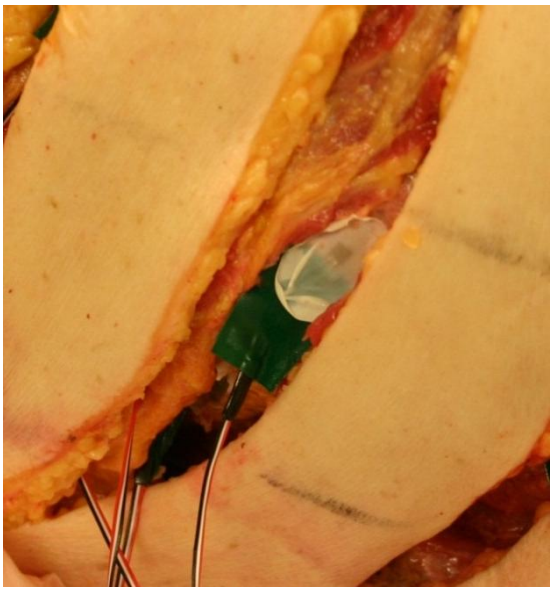

Figure 10: Installation of a middle strain gauge

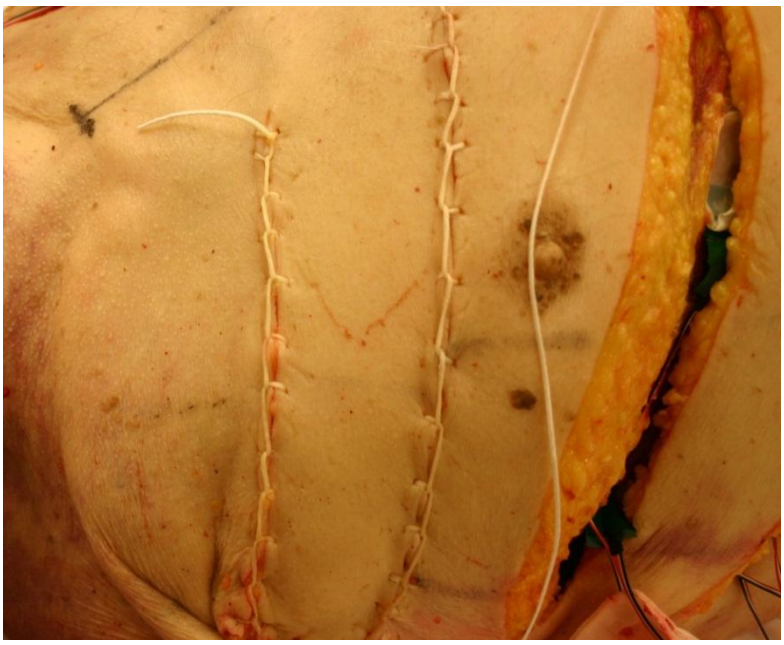

Figure 11: Rib incisions sutured closed after installation of strain gauges

The strain gauge leads were arranged in a configuration during closure of the incision to relieve the strain on the gauges as best as possible. The PMHS subject was rotated from a supine to a prone position for installation of the posterior strain gauges. The same procedure was followed for the application of the posterior strain gauges. All posterior strain gauges were

applied at the costal angle on the rib. The PMHS subject was then stored overnight in a cooler prior to testing.

PMHS Testing

For testing, the PMHS subject was arranged in the upright seated position. The head was suspended using a cervical sling, keeping the subject in the proper upright orientation. The PMHS' knees were also strapped flush with the testing platform to ensure the subjects' hips were properly aligned with the orientation of the shoulders.

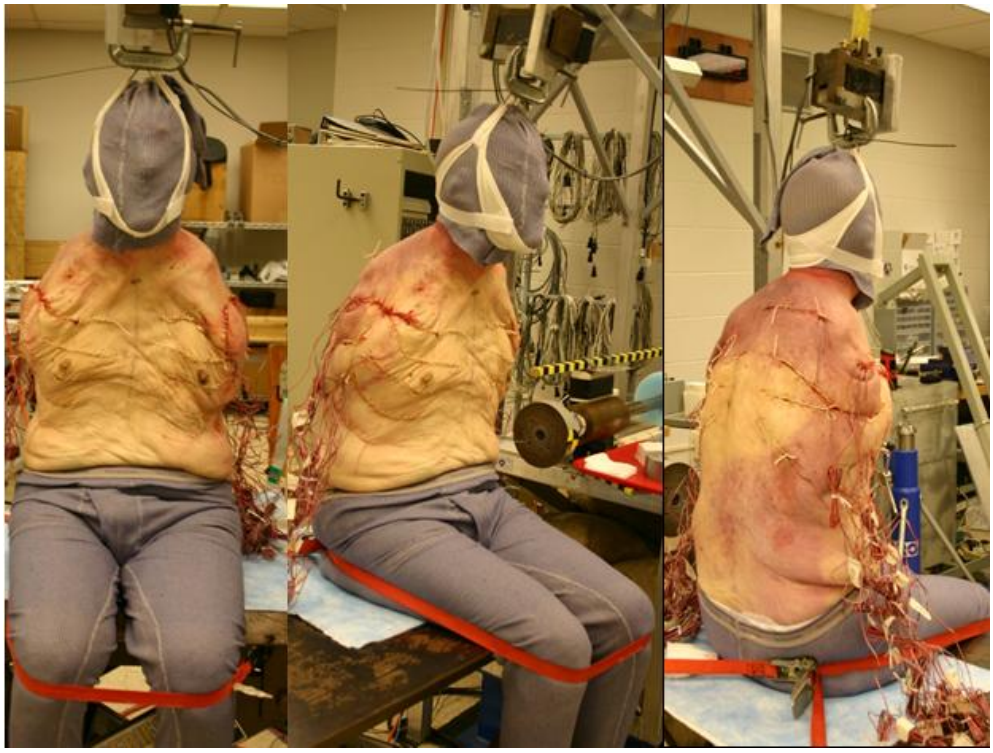

(a) (b) (c)

Figure 12: PMHS Subject in seated position (a) anterior view

(b) Anterior oblique view (c) oblique view

The trachea was prepped for installation of a trachea tube. The incision for the trachea was enlarged and larynx was pulled out to ensure proper connection and so a seal could be created when the respiration pump was used. This trachea preparation can be seen in Figure 13. The trachea tube was inserted and a balloon at the distal end of the tube was filled to create a seal. The seal was produced to inhibit air from escaping the lungs. A manual respirator pump with pressure gauge was attached to the trachea tube for pumping air into the lungs to mimic respiration. Figure 14 shows the pump attached to the trachea tube.

Figure 13: Preparation of the trachea

Figure 14: Application of the respiration pump to the installed trachea tube, anterior oblique view

All strain gauges were attached to the Yokogawa data acquisition system. All gauges were again checked for proper working condition. The chest band was attached to the data acquisition system at this time and was balanced in the same manner as previously mentioned in the '*in vivo*'

methods section. The Yokogawa data acquisition system was set to capture data at 1000 Hz for 2 minutes. Prior to initiating the first test sequence, the temperature of the PMHS subject was taken by placing a thermometer lead down the trachea tube into the lungs. The initial temperature of the PMHS was 46□F while the ambient room temperature was 74□F.

PMHS Respiration Simulation Procedure

Eight respiration sequences were created under slightly different boundary conditions. Table 1 shows the test matrix for all eight tests conducted. This comprehensive table includes the pressure differential used to simulate the breaths, the quantity at each level, and how the respirator bag was manipulated after achieving the desired pressures.

Table 1: Respiration Trial Test Matrix

Test Number	Breath Pressure Differential (cm H_2O)	Breath Repetitions	Respirator Bag Removal (Y or N)
Test 1			
	20	5	N
	90	1	Y
	20	xx	xx
Test 2			
	20	2	N
	90	3	Y
	20	3	Y
Test 3			
	20	4	Y
	90	5	Y
	20	4	Y
Test 4 and 5 (chest band)			
	20	4	Y
	90	4	Y
	20	4	Y
Tests 6,7, and 8			
	30	4	Y
	100	4	Y

	30	4	Y

The first test was performed by attaching the respiratory bag and simulating shallow breathing by creating a 20 cm H_2O pressure difference between the inside of the lungs and atmospheric pressure. After the desired pressure inside the lungs was reached, the pump operator ceased pumping until the pressure inside the lungs had gradually diffused back out through the respiratory pump. This procedure was repeated five times to mimic shallow or normal breathing. The pressure differential was then increased to 90 cm H_2O to simulate deep breaths. After the 90 cm H_2O pressure differential was obtained, the respiration pump was removed from the trachea tube to allow for a faster exhalation rate. For the first trial, due to the low exhalation rate through the pump, only five shallow breaths and one deep breath were able to be captured due to data acquisition time constraints.

The second trial repeated the same procedure as above for inflating the lungs. The breathing sequence for the second test was two breaths at a pressure difference of 20 cm H_2O (small breaths), not removing the respirator pump, followed by three breaths at a pressure difference of 90 cm H_2O (deep breaths), removing the pump after the target pressure was obtained, and then repeating three of the 20 cm H_2O breaths, and removing the pump again after the target pressure was obtained. After this test, the data acquisition time was reduced to 90 seconds.

The third trial consisted of four small breaths, five deep breaths, followed by another four small breaths and removing the respirator pump after each targeted pressure was obtained.

For trials four and five, the chest band was placed on the subject. The chest band was positioned using a laser level and can be seen in Figure 15. The location of the band was

recorded by noting the strain gauge number on the band relative to anatomical locations of the spine and sternum, as in the *in vivo subject* (Appendix A). The breathing pattern pressures from the previous trials were repeated with the chest band strapped to the PMHS.

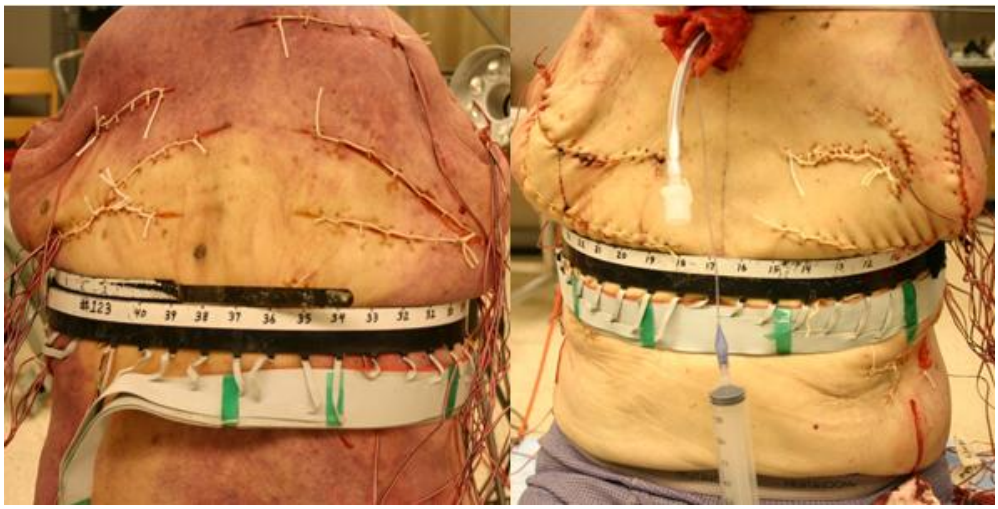

(a) (b)

Figure 15: Posterior (left) and anterior (right) view of applied chest band

For tests six thru eight, the chest band was removed and the pressure differentials were increased. Shallow breaths were simulated at a pressure differential of 30 cm H_2O and the large breaths were simulated at a pressure differential of 100 cm H_2O. The test respiration cycle consisted of obtaining four small breaths, four large breaths, followed by another four small breaths at the previously mentioned pressures. The respiration pump was removed and reattached after the desired pressures were obtained.

During test seven, the testing was halted due to a buildup of mucus within the trachea tube. This blockage was inhibiting the escape of air from the lungs after the respirator bag was detached. Test 8 was then performed, but once again halted due to excessive mucus blockage in the trachea tube. Furthermore, it was seen that air had begun entering the abdominal cavity,

suggesting that a lung had ruptured. This prohibited testing to continue. The following methods section will discuss the procedures used to analyze the data.

Data Analysis

To analyze the data, the magnitude of the strain was taken from the various peaks that occurred from simulating respiration on the PMHS. To obtain the magnitude of change of strain that occurred, all gauges were zeroed based on the initial steady state readings of the gauge data. From this, the maximum and minimums between respiration simulations were taken. The magnitude of this difference was taken to be the change of microstrain.

$$strain\ magnitude = |maximum - minimum|$$

This was performed for individual peaks simulated by the respiration pump including the initial small breaths, the large breaths, and the recovery small breaths. An example of the zeroed signal with the different minimum and maximum points can be seen in Figure 16.

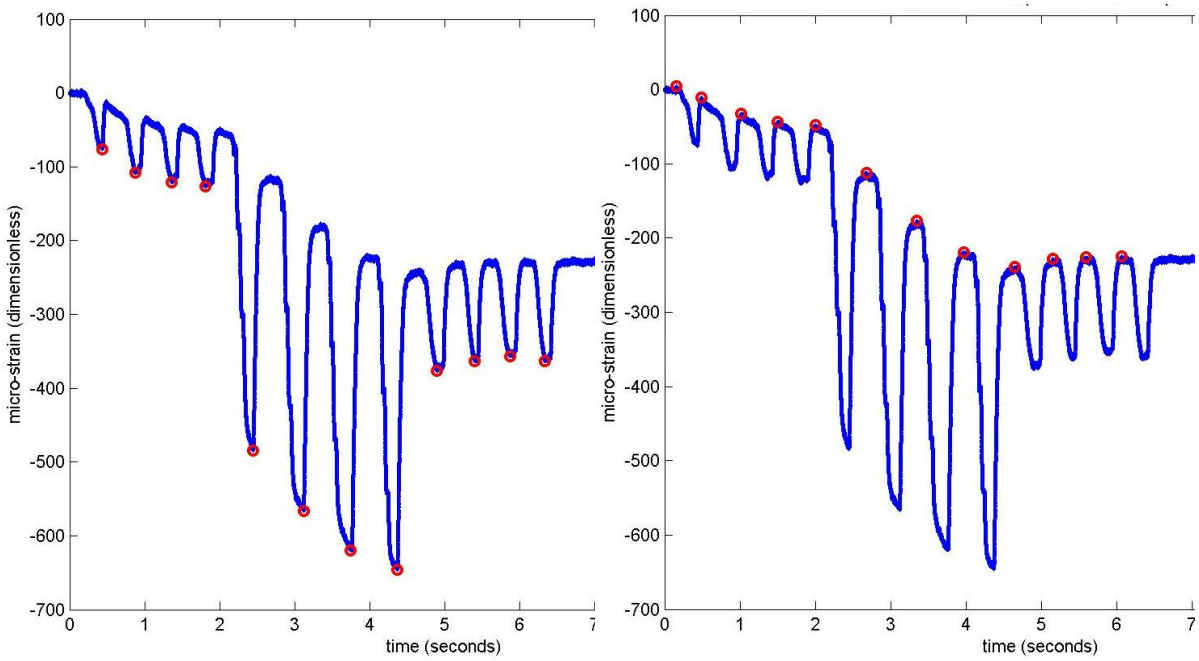

Figure 16: Sample min (left) and max (right) points used to evaluate micro-strain magnitude

These points were collected for each of the runs and grouped accordingly to the previously mentioned test conditions. It should be noted that these magnitudes were taken only for tests 2,3,4,5 and 6.

Results: Comparing PMHS respiration simulation to *in vivo*

Figure 17 thru Figure 20 represent a sample of the chest band data collected from the breathing exercise performed by the *in vivo* subject and from the simulated respiration data with the PMHS. Orientation of the chest band for both the PMHS and *in vivo* subjects are shown in Appendix A. Figure 17 and Figure 18 show clear peaks for both the PMHS data and the *in vivo* data.

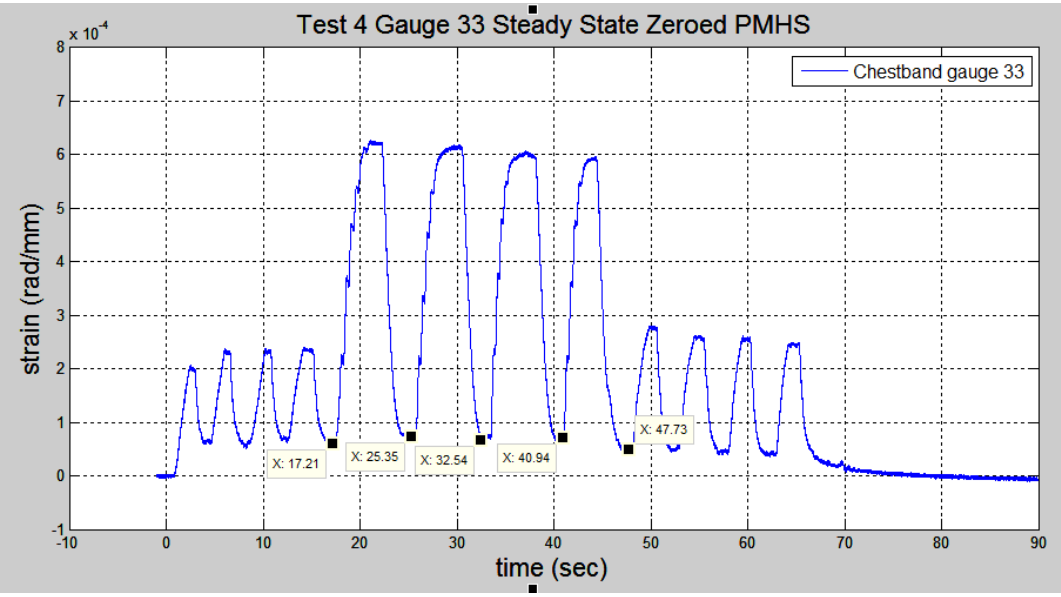

Figure 17: PMHS chestband data sample from Test 4, gauge 33; data has been steady state zeroed

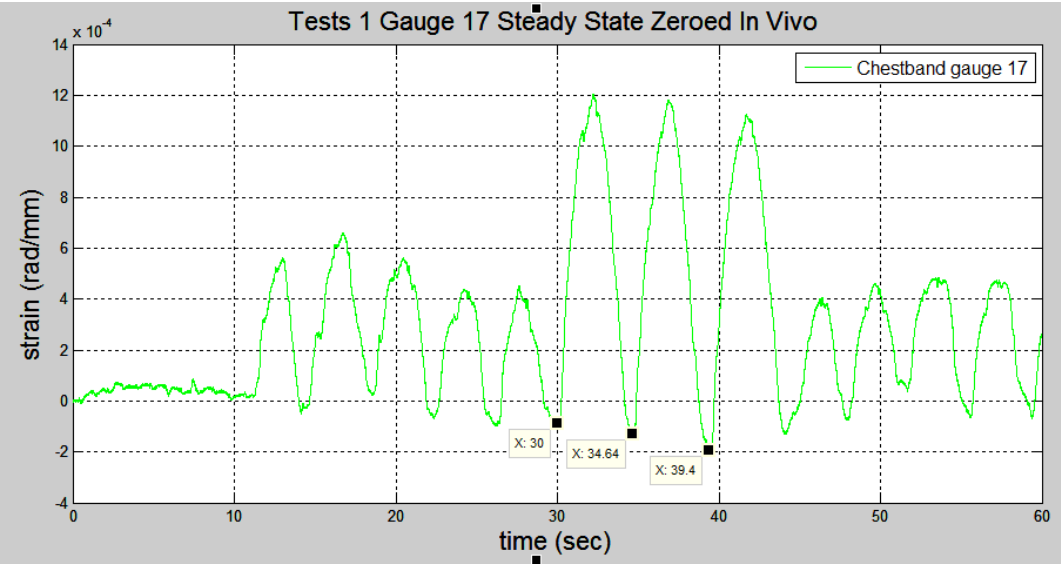

Figure 18: *In vivo* chestband data from Test 1, gauge 17; data has been steady state zeroed

Using only the deep inhalations as a reference, Table 2 was constructed to assess the time interval each breath took to manifest.

Table 2: Inhalation-Exhalation time interval comparison between PMHS and *in vivo*

Subject	**T1 (seconds)**	**T2 (seconds)**	**Δ*T*(seconds)**
PMHS	17.21	25.35	8.14
PMHS	25.35	32.54	7.19
PMHS	32.54	40.94	8.4
PMHS	40.94	47.73	6.79
Average PMHS			7.63
In vivo	30.00	34.64	4.64
In vivo	34.64	39.40	4.76
In vivo	39.40	44.13	4.73
Average *In vivo*			4.71

The PMHS experimental setup took approximately three seconds longer to generate a deep inhalation-exhalation cycle than the *in vivo* subject. The PMHS and *in vivo* subject experienced

similar data signals at a comparable anatomical location. The gauge on the sternum for both the PMHS (gauge 17) and the *in vivo* (gauge 21) are shown in Figure 19 and Figure 20.

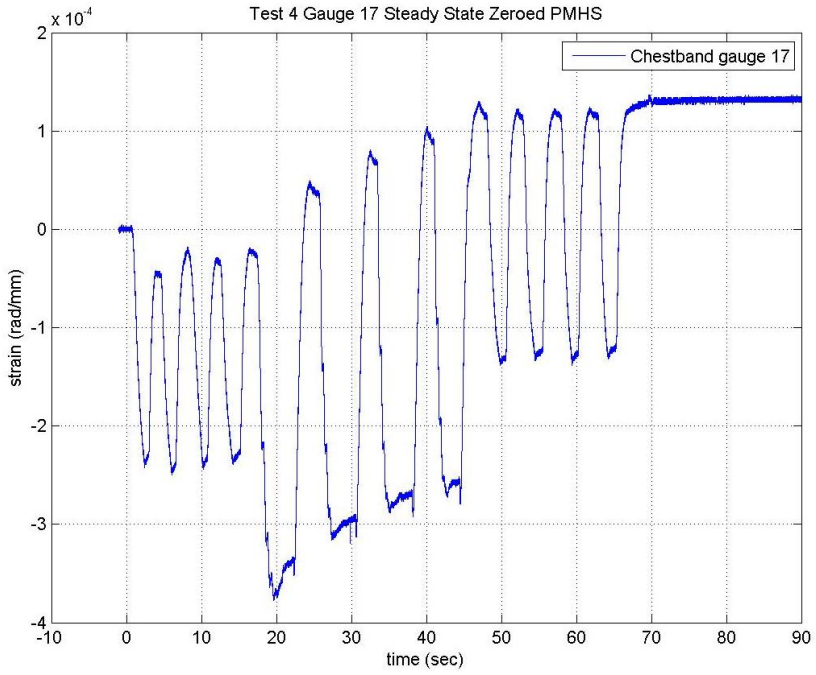

Figure 19: PMHS sternum gauge 17, Test 4; data has been steady state zeroed

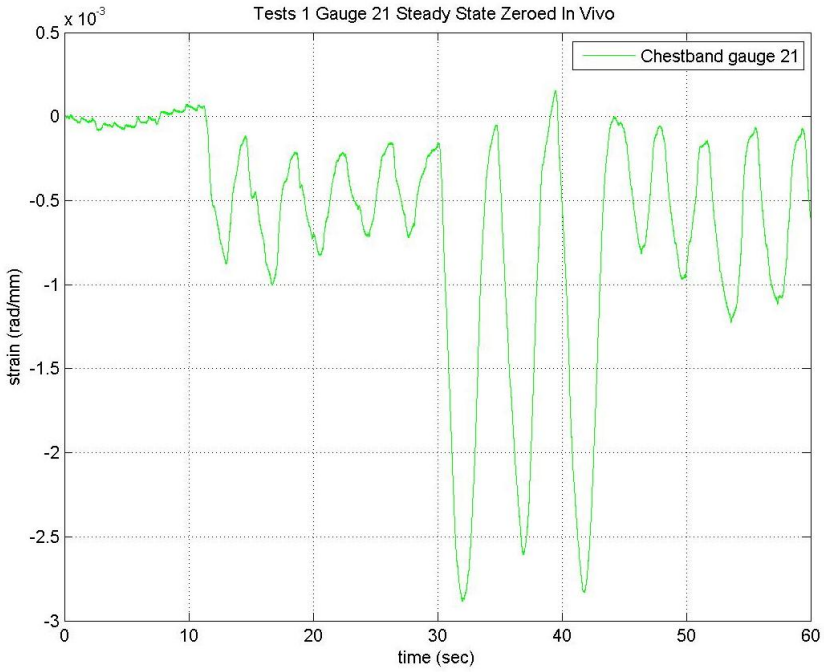

Figure 20: In vivo sternum gauge 21, Test 1; data has been steady state zeroed

Results PMHS

Several tests from the planned test matrix were not included in the analysis. The exclusion of each of these tests will be explained. Test 1 was not included in any analysis because it was an initial test used to validate experimental setup. When analyzing the different peaks, Test 2's initial small breath peaks were not included because the respirator pump was not pulled off the trachea tube. The peaks not included in Test 2 can be seen below in Figure 21, highlighted by the blue shaded box. These peaks were not included in the data analysis because the exhalation rates were slow and not representative of the *in vivo.*

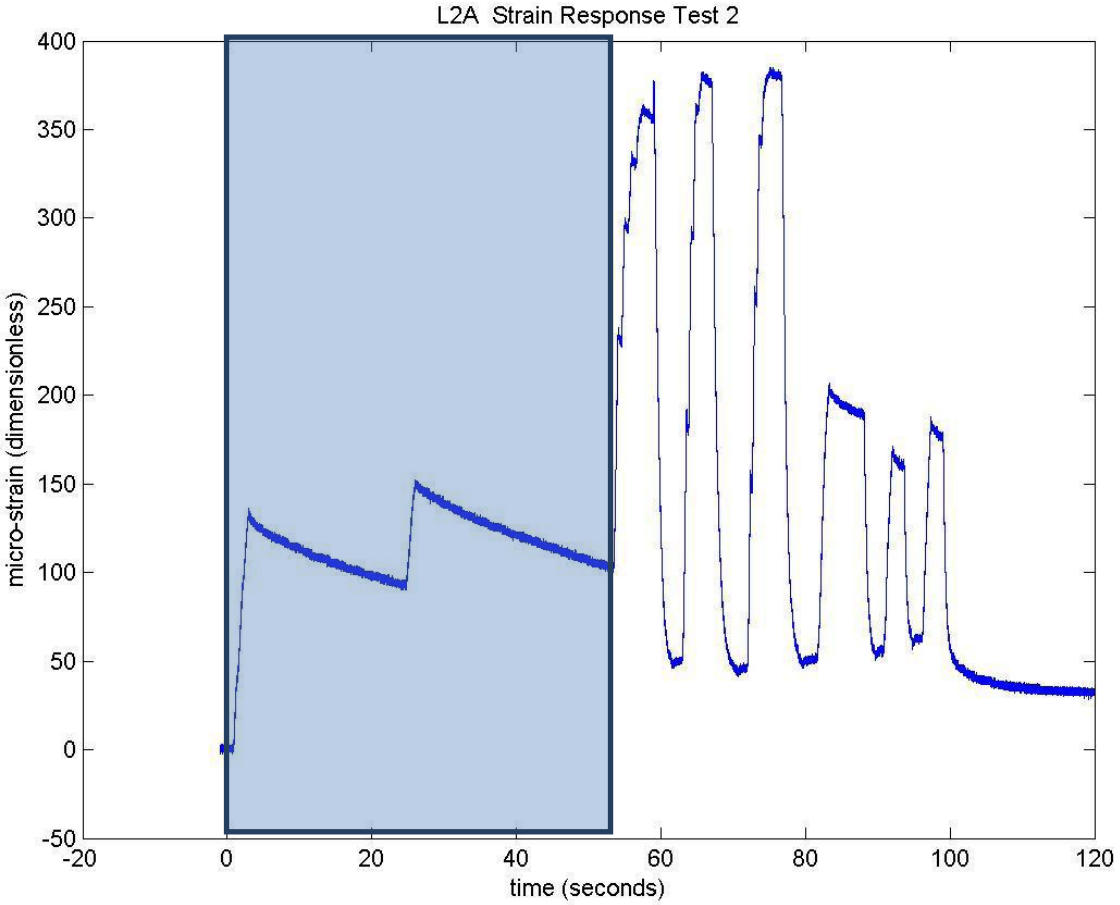

Figure 21: Slow exhalation strain response

Tests 7 and 8 were not included in the analysis due to blockage of the trachea tube caused by the buildup of phlegm. Figure 22 shows the response of two strain gauges exhibiting phlegm blockage. The blockage has been highlighted with a yellow box.

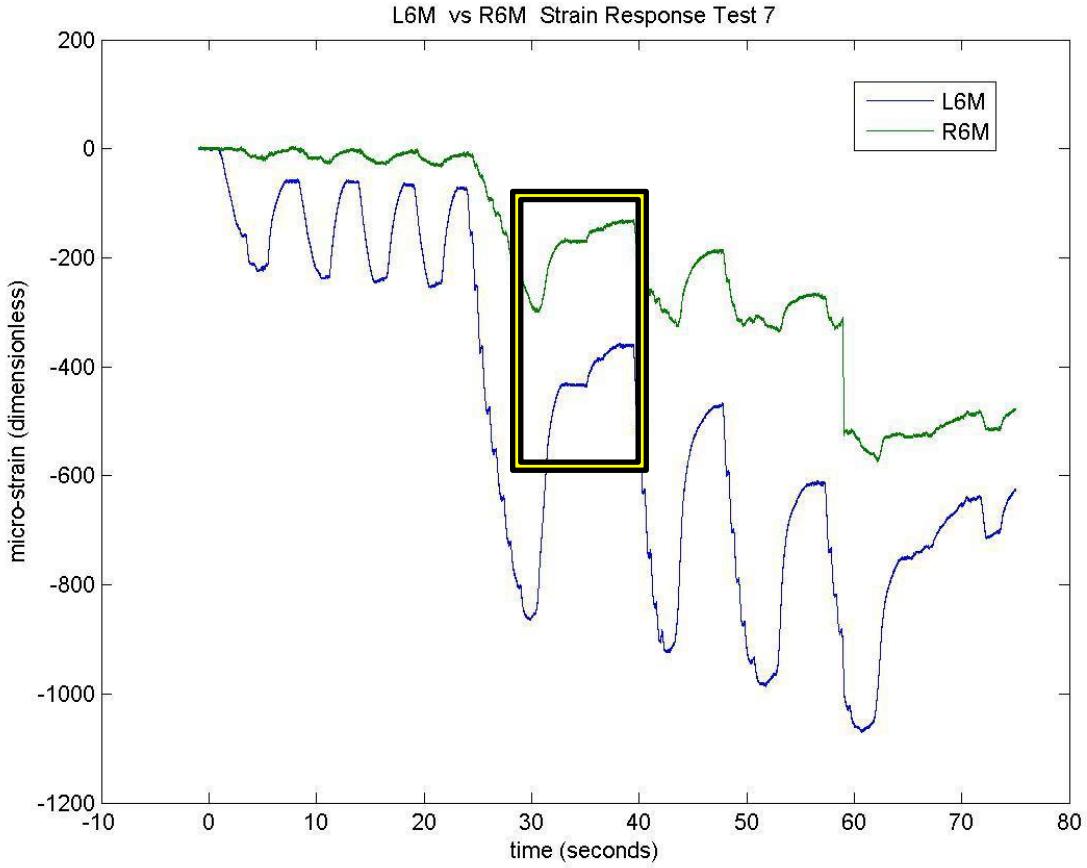

Figure 22: Strain response caused by phlegm build up

Test 8 was excluded because it appeared one or both of the lungs had ruptured. This was based on a visual of air beginning to fill the PMHS abdominal cavity and confirmed as exhalation of the PMHS did not result in a corresponding strain drop but a continual strain from the air that

escaped the ruptured lung. Figure 20 below shows the continual buildup of pressure on both ribs due to air escaping into the abdominal cavity.

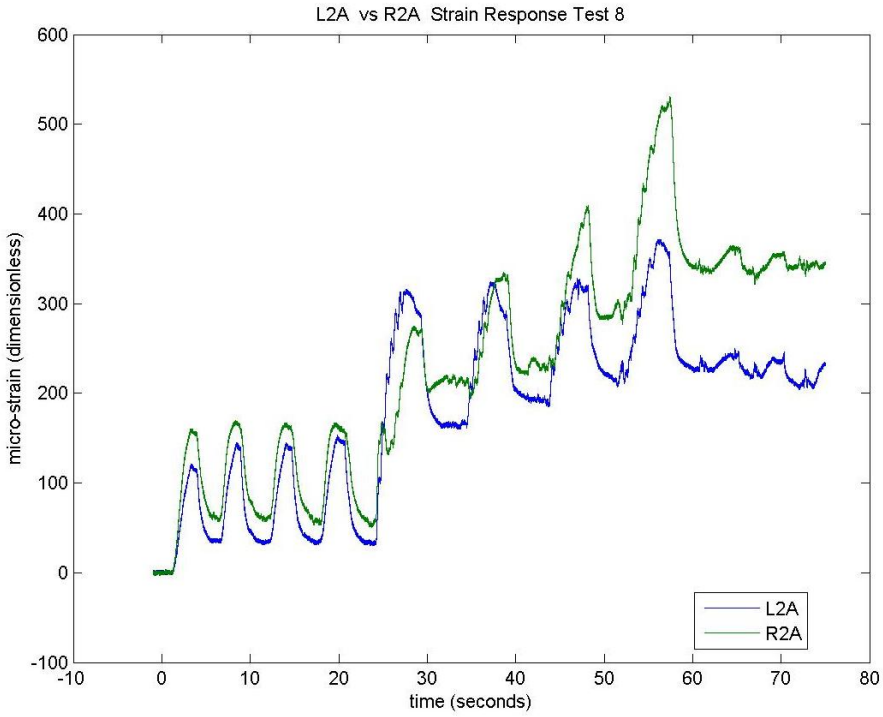

Figure 23: Continual strain build up from ruptured lung

The remainder of the data was used to calculate the magnitudes of the peaks. Tests 2, 3 and 6 are compared to each other based on similar boundary conditions. Tests 4 and 5 are compared to each other as well because the chestband was placed on the PMHS. The peaks will be analyzed for trends superior to inferior by strain gauge location, by rib and strain gauge location, and by comparing both the right and left sides by rib and strain gauge location.

The data collected from the PMHS with the chestband attached(Test 4 and Test 5) will be used to compare the breathing pattern of the *in vivo* subject as compared to the breathing pattern created in the experimental setup.

Comparison of PMHS Tests 2, 3, and 6

Tests 2, 3 and 6 were grouped together because they were all tests where the pressure differentials used to simulate respiration were the same and the chest band was not on the PMHS. Figure 24 shows the spread of microstrain from all of the gauges recording the large breath magnitudes derived from Tests 2, 3 and 6. All of these magnitudes were determined for the large breaths, which were simulated at a pressure differential of 90 cm H_2O. These individual graphs compare both the left and right side, rib number, and anantomical location.

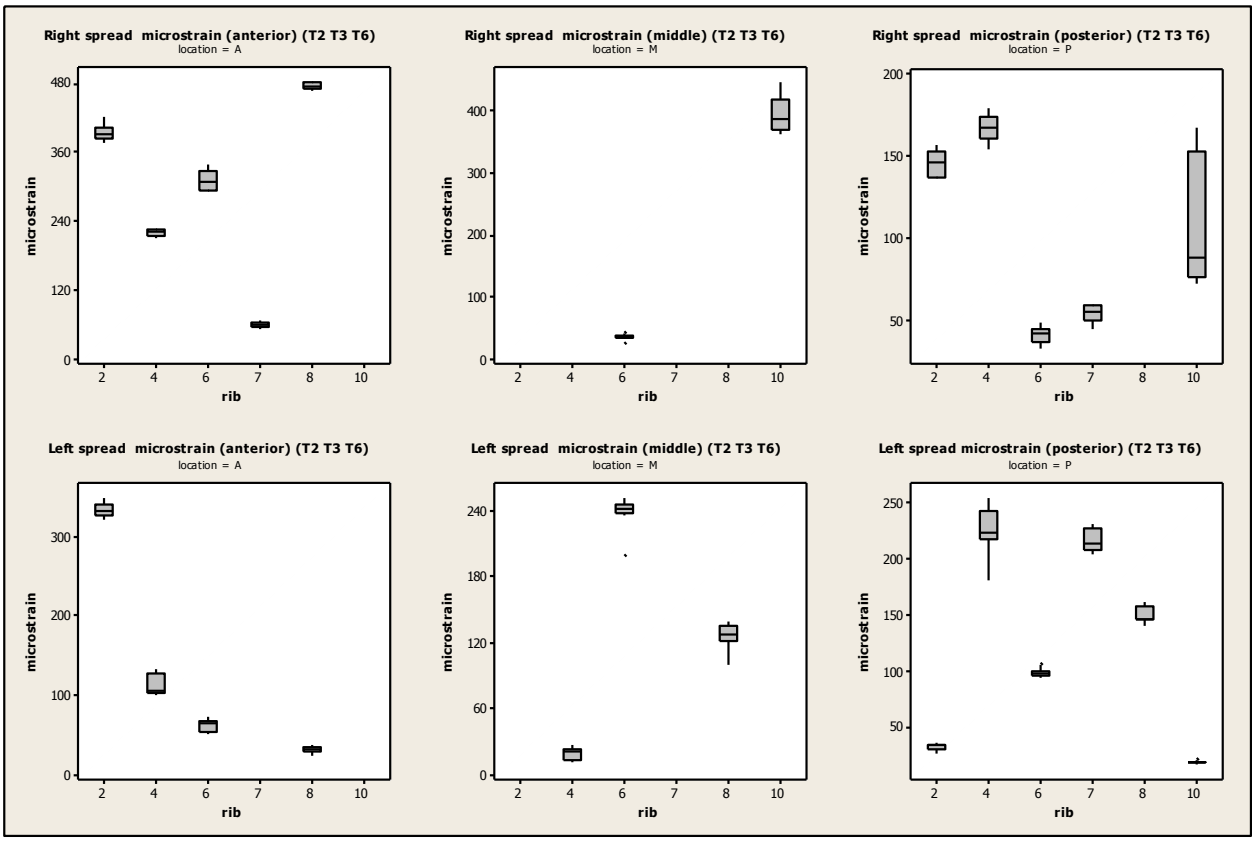

Figure 24: Boxplot spread of large breath magnitudes for left and right gauges by anterior, middle and posterior locations from Tests 2, 3, and 6

As can be seen in Figure 24, some gauges [specifically the right middle, rib 10 (RM10) and the right posterior, rib 10 (RP10)] had significant variability. The experimental points from Test 6 were determined to be the cause of this spread. Test 6 was removed to analyze the repeatability of the experimental setup. The boundary conditions were changed after Test 2 and 3 because the chest band was added for Tests 4 and 5, and then removed chest band for Test 6. The addition and removal of the chestband caused significant strain gauge variation. After removing Test 6, the spread of the microstrains for each of the gauges is show in Figure 25.

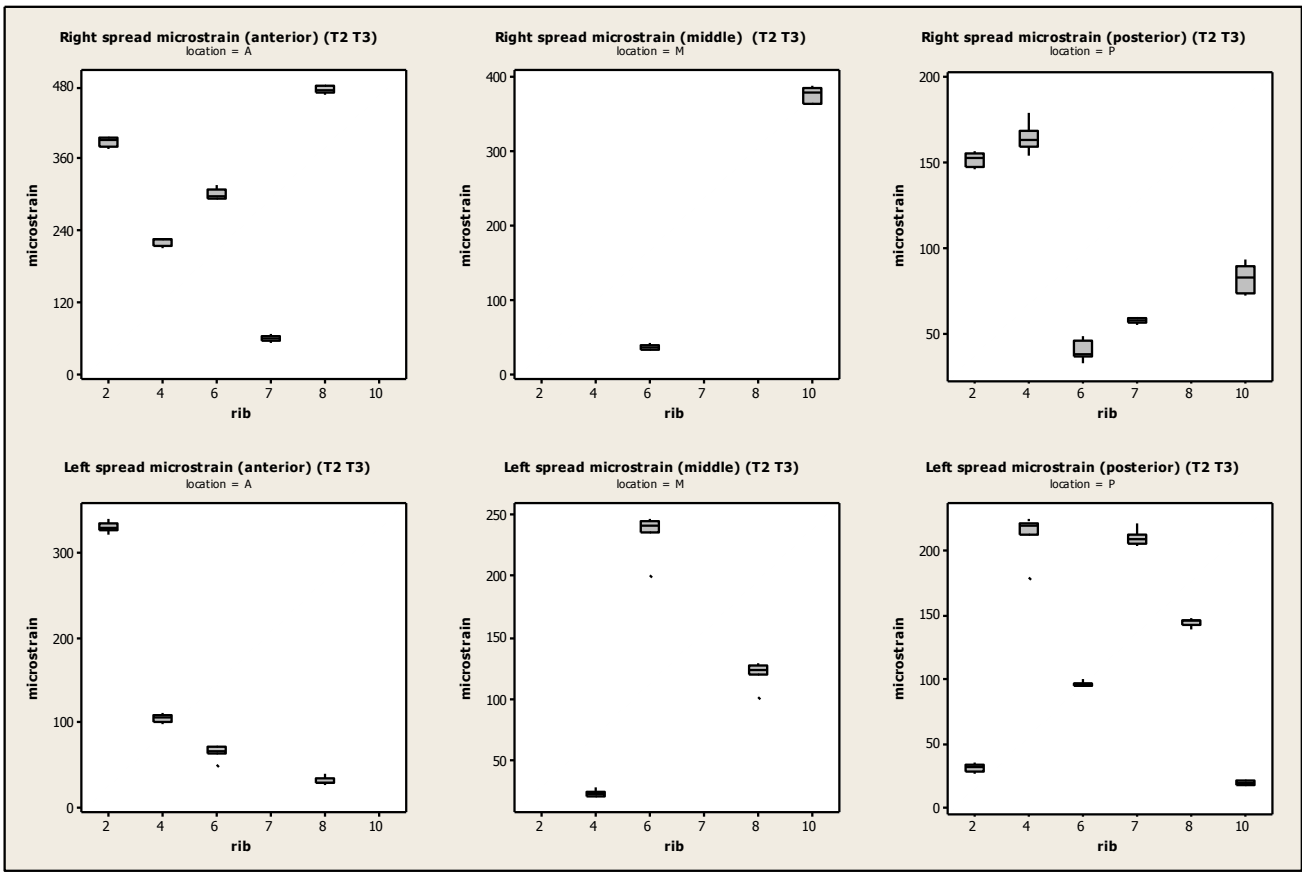

Figure 25: Boxplot spread of large breath magnitudes for left and right gauges by anterior, middle and posterior locations from Tests 2 and 3

Using the cumulative data for all rib gauges on both the right and left, the microstrain amplitudes were evaluated by location for any locational trends. The box shown in Figure 26 reveals statistical difference in the anterior vs. middle and anterior vs. posterior. However, it does not show statistical difference in the middle vs. posterior locations. The resulting p-values of the Tukey-Kramer comparisons can be seen in Table 3.

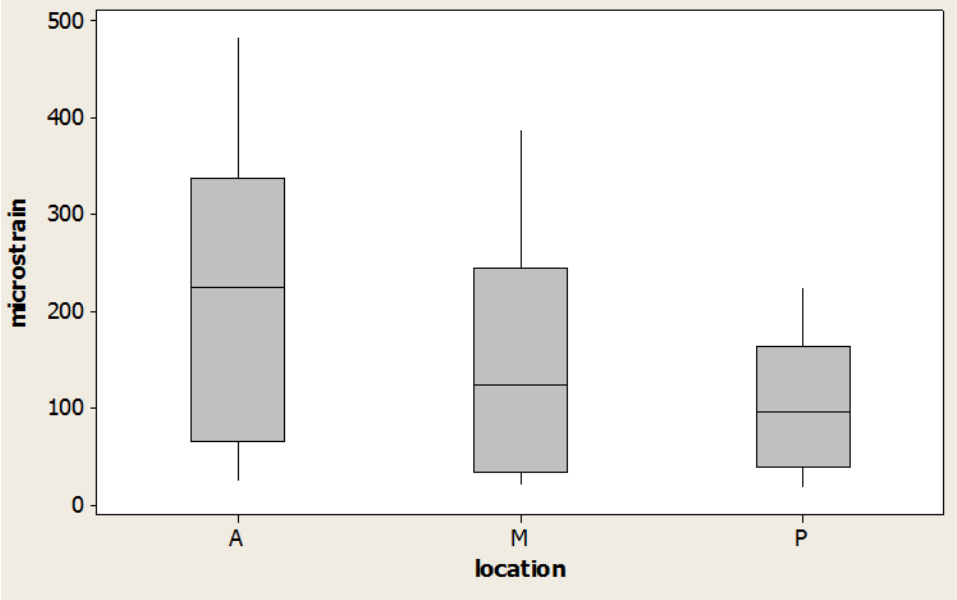

Figure 26: Microstrain spread by locations (Anterior-A, Middle-M, Posterior-P); spread includes both the right and left gauges for all instrumented ribs (2, 3, 4, 6, 7, 8, and 10) for both Tests 2 and 3

Table 3: Tukey-Kramer comparison p-value results 95% CI (*denotes statistical difference)

Level	**Level**	**p-value**
Anterior	Posterior	<0.0001*
Anterior	Middle	0.0331*
Middle	Posterior	0.1052

Per the procedure described in the methods section, the following average rib microstrains were obtained for each gauge. It should be noted that an 'x' in the figure denotes a strain gauge that was damaged or malfunctioned during experimentation. Figure 27 and Figure 28 report the average magnitudes of the three different gauge locations (A, M, P) on the appropriate instrumented rib. Due to the large number of failed gauges (particularly in the medial), no trends could be reported across the rib body of any particular rib.

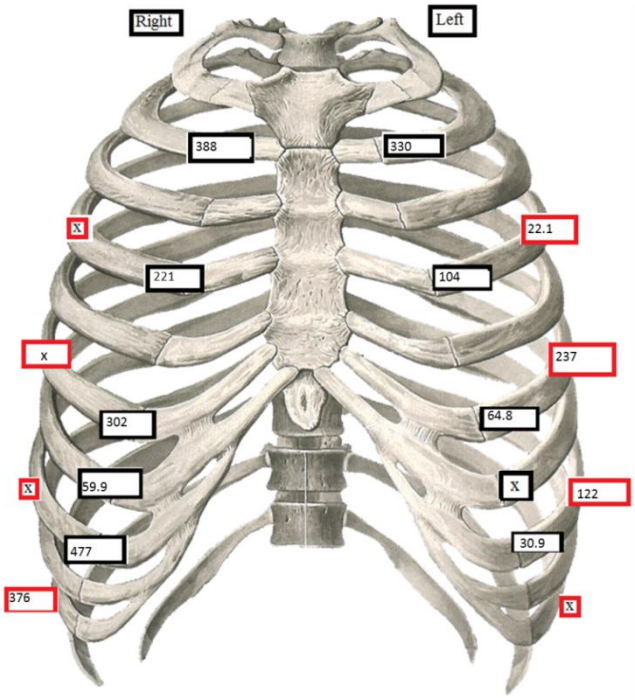

Figure 27: Test 2 and 3 anterior and middle gauge microstrain amplitudes

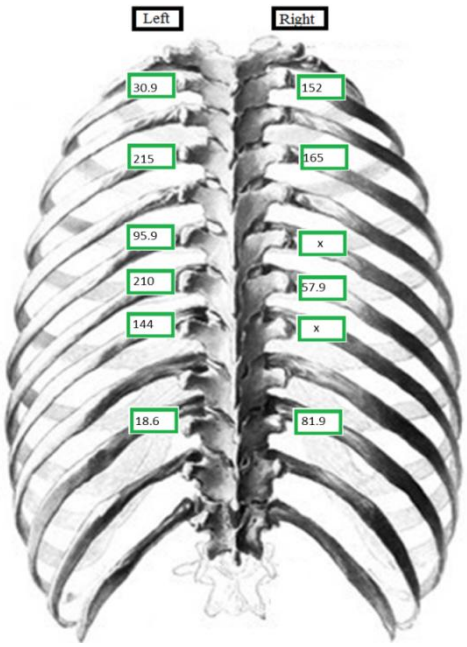

Figure 28: Test 2 and 3 posterior gauge microstrain amplitudes

Microstrain amplitude was also analyzed for trends in regards to inferior to superior and by anatomical location. Figure 29 shows a stacked display of the strain by location versus the rib number for the right side. The right side exhibited consistently greater strain anteriorly on ribs 2, 4, 6 than posteriorly. Rib 8 displayed the highest average microstrain of 477 on the right side. No trend was determined for anterior, middle or posterior, displaying an increasing or decreasing magnitude value in the superior to inferior direction.

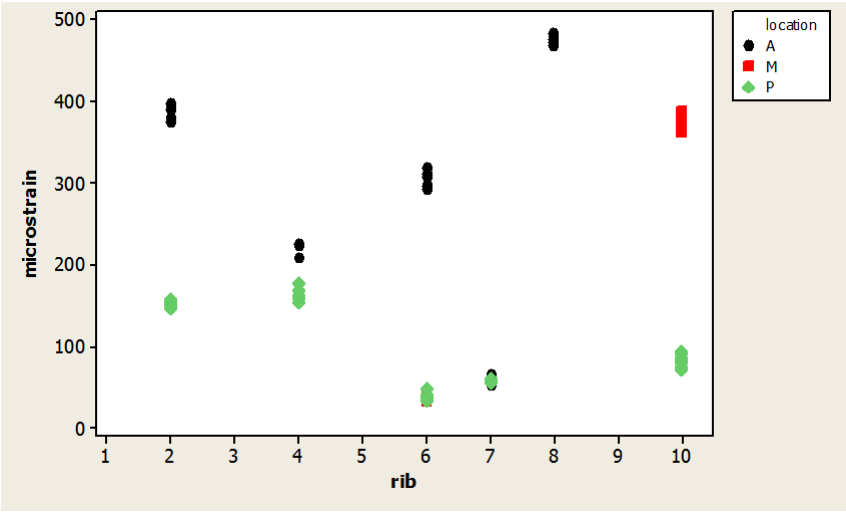

Figure 29: Right stack scatter of microstrain by rib and location for test 2 and 3

Figure 30 shows a stacked display of the strain by location versus the rib number for the left side. The left side did not exhibit the same trends as the right side. The left side displays a rough trend of decreasing strain amplitude anteriorly in the superior to inferior direction of the rib cage. The left and right side did not display consistent trends quantifying a particular higher strain magnitude by location. The left side did not display the anterior location as predominantly higher as the right side data suggested.

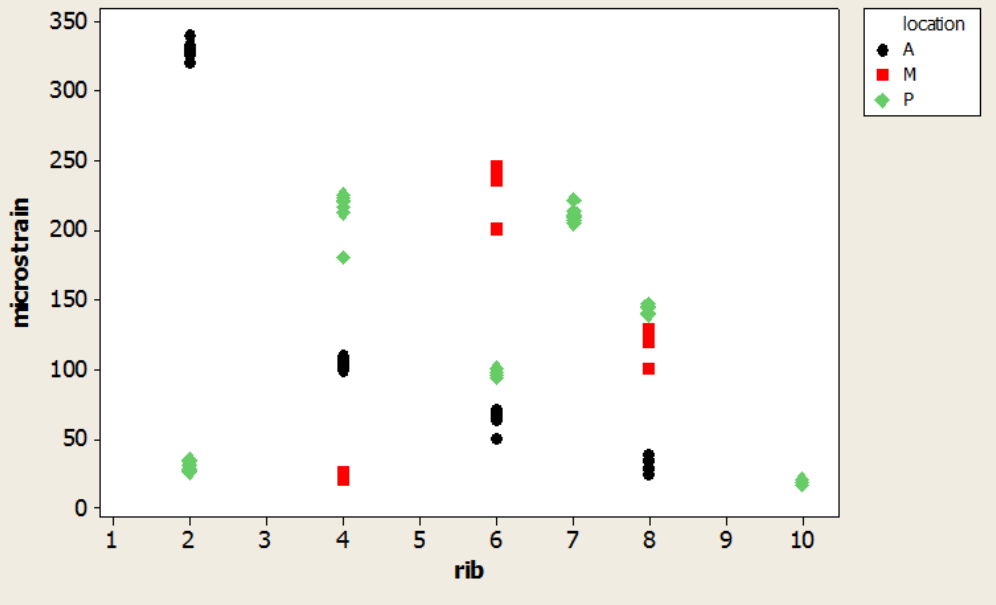

Figure 30: Left stack scatter of microstrain by rib and location for test 2 and 3

The following plots and figures show the results from the PMHS with the chestband attached. The repeatability of the gauges with the chestband applied can be seen in Figure 31. The left side instrumentation exhibited much more repeatable results. The variation that is seen in locations R10M and R10P are similar to the variation that was seen in Test 6. The variations stem directly from application of the chestband which chestband predominately increased the microstrain magnitude. The comparison for each location (anterior, middle, and posterior) with the chestband applied and not applied can be seen in Figure 32-Figure 34Figure 33.

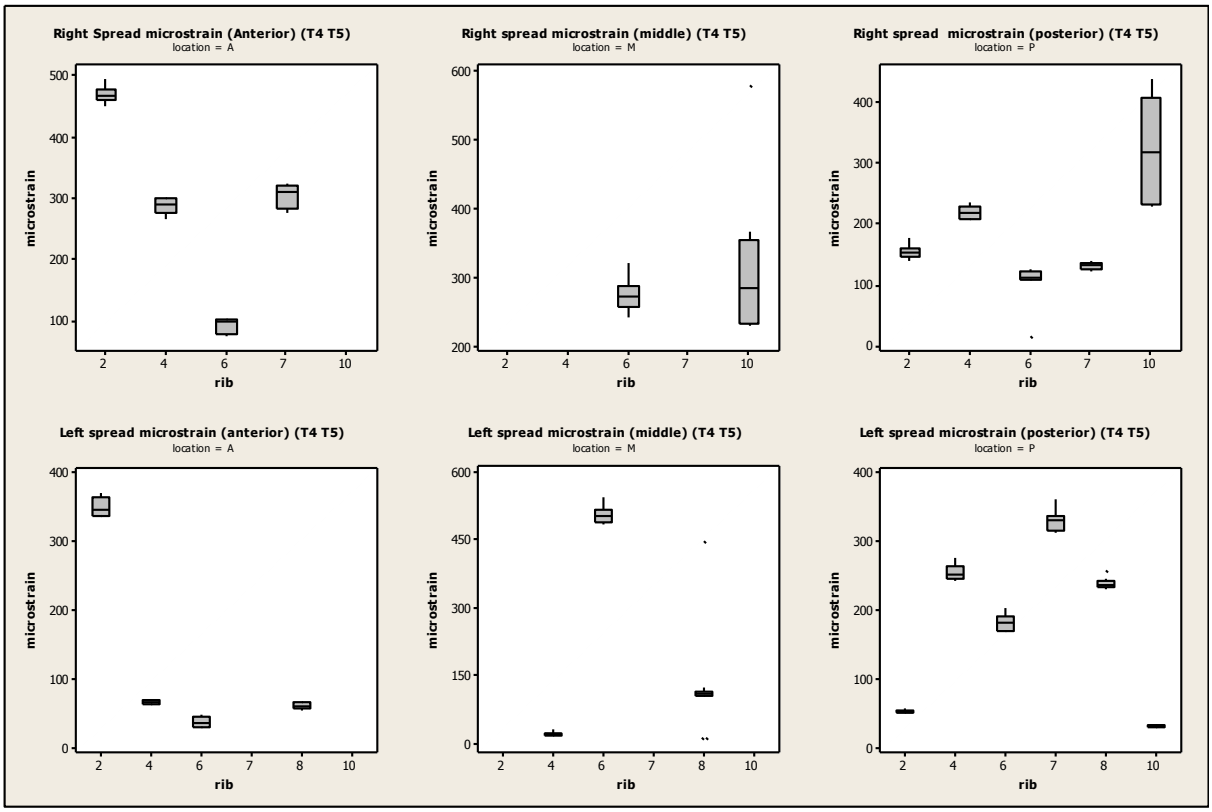

Figure 31: Chestband applied microstrain data repeatability

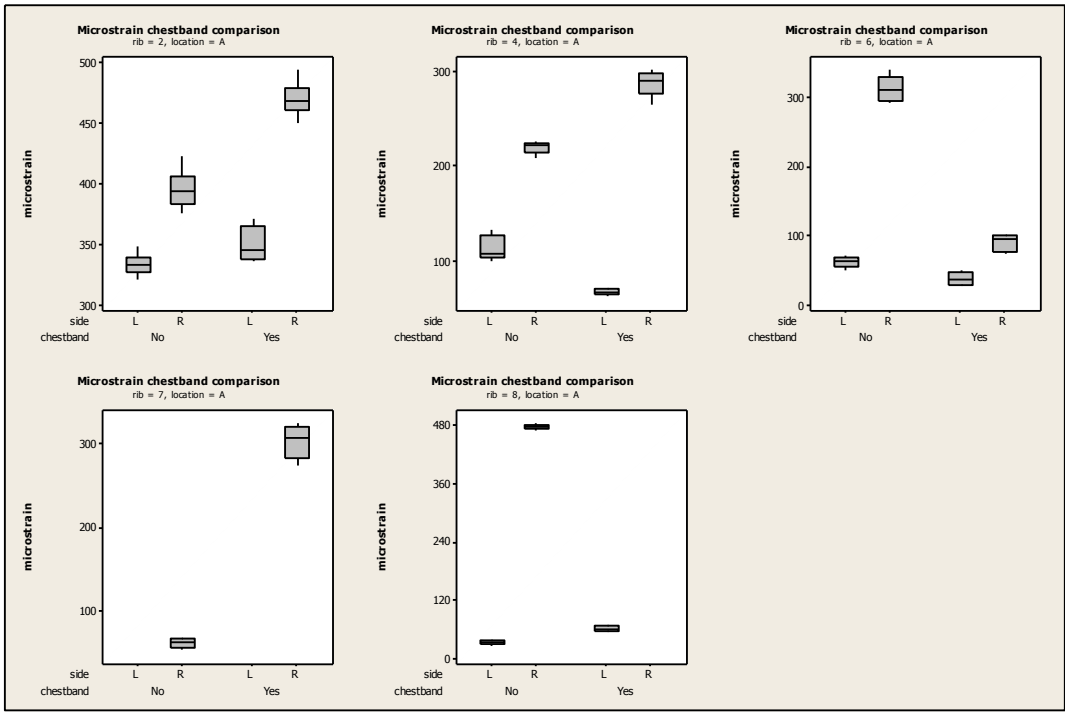

Figure 32: Anterior gauge microstrain chestband comparison

As can be seen in Figure 32, R2A and L2A experienced an increase in microstrain with the chestband applied. On rib 4, L4A experienced a drop in microstrain whereas R4A increased. Both the right and left anterior rib 6 experienced a drop in microstrain (R6A and L6A). Both locations R7A and L10A experienced an increase in microstrain. It can also be seen that application of the chestband caused gauge R8A to malfunction.

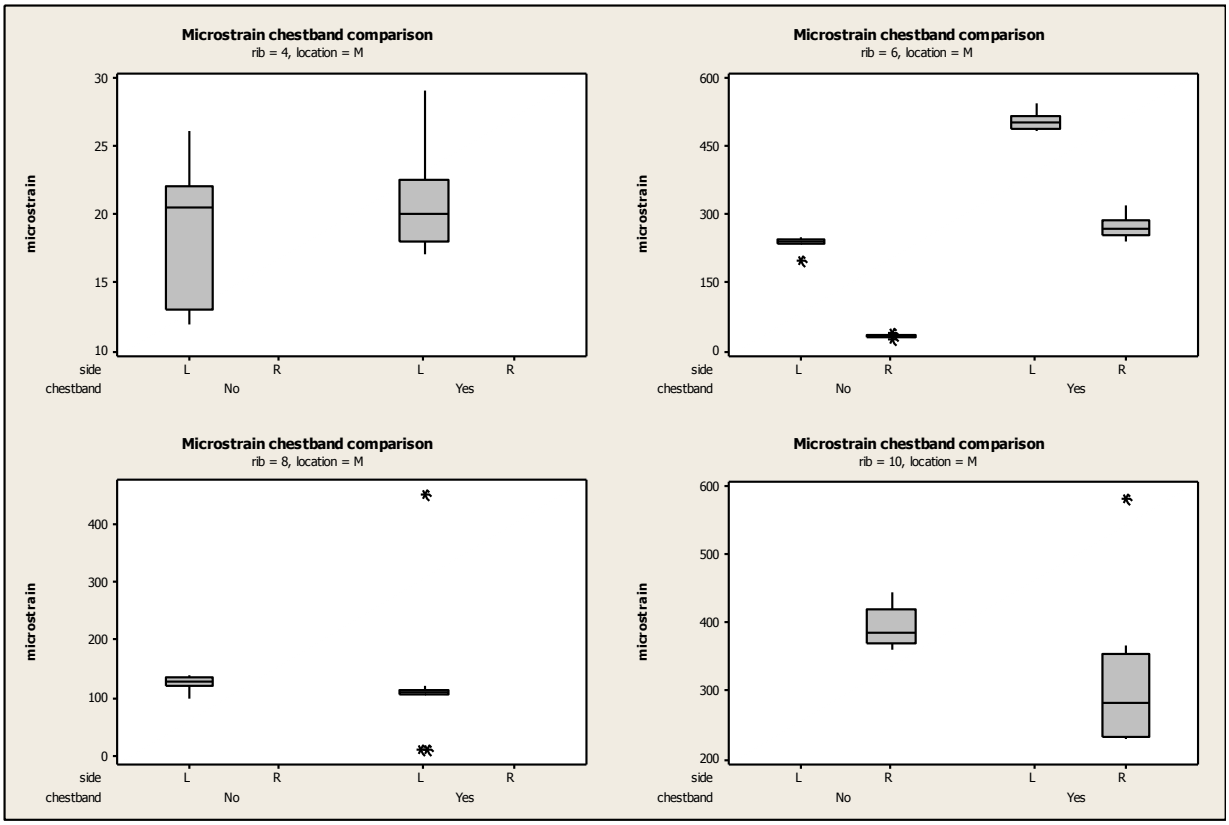

Figure 33: Middle gauge microstrain chestband comparison

The changes for the middle location with the chestband vary substantially. L4M and L8M experienced little change. L6M and R6M both experienced an increase in microstrain. R10M experienced a drop in microstrain.

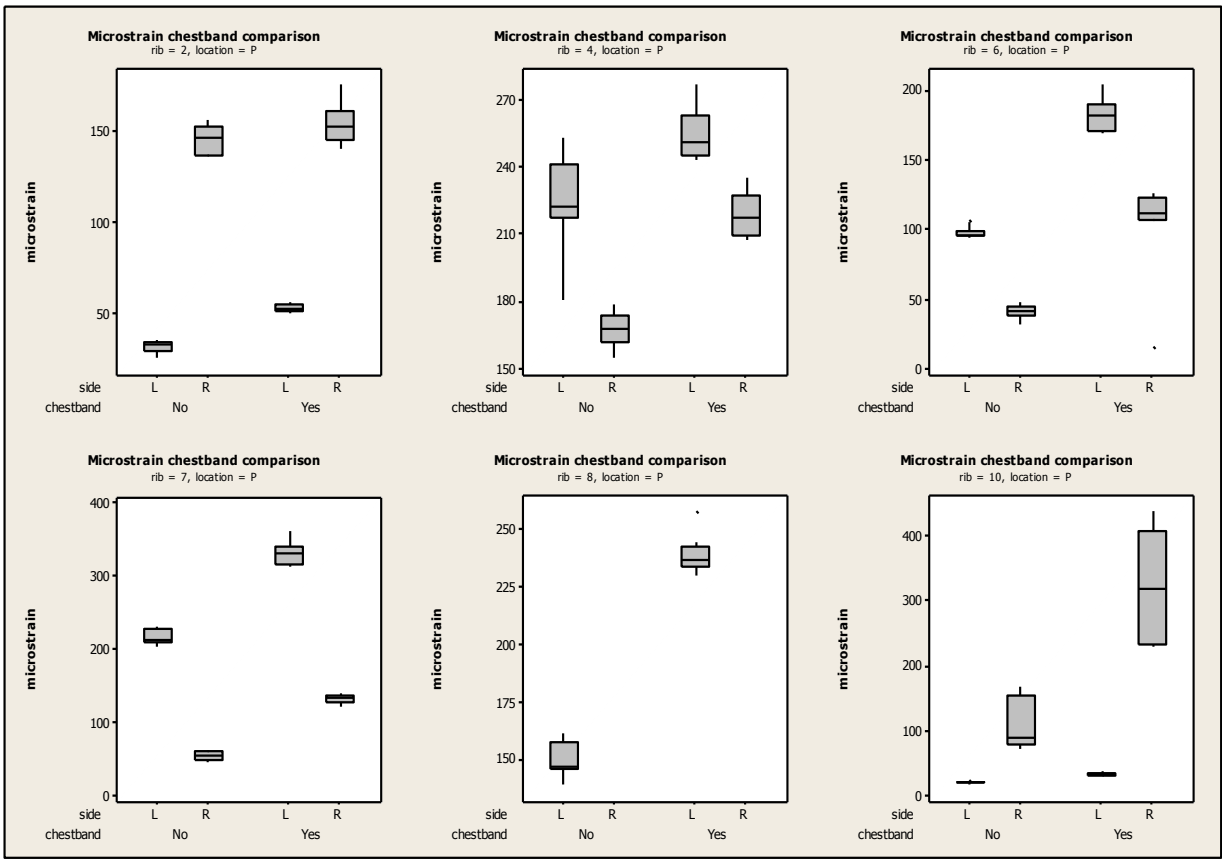

Figure 34: Posterior gauge microstrain chestband comparison

The posterior gauges all experience an increase in microstrain with application of the chestband.

The following table summarizes the change in strain experienced by each of the gauges.

Table 4: Left/ Right location chestband application comparison

Rib	Anterior		Middle		Posterior	
	Left	Right	Left	Right	Left	Right
2	+	+	n/a	n/a	+	+
4	-	+	≈	n/a	+	+
6	-	-	+	+	+	+
7	n/a	+	n/a	n/a	+	+
8	+	n/a	≈	n/a	+	n/a
10	n/a	n/a	n/a	-	+	+

Figure 35 and Figure 36 report the average magnitudes of the three different gauge locations (A, M, P) on the appropriate instrumented rib.

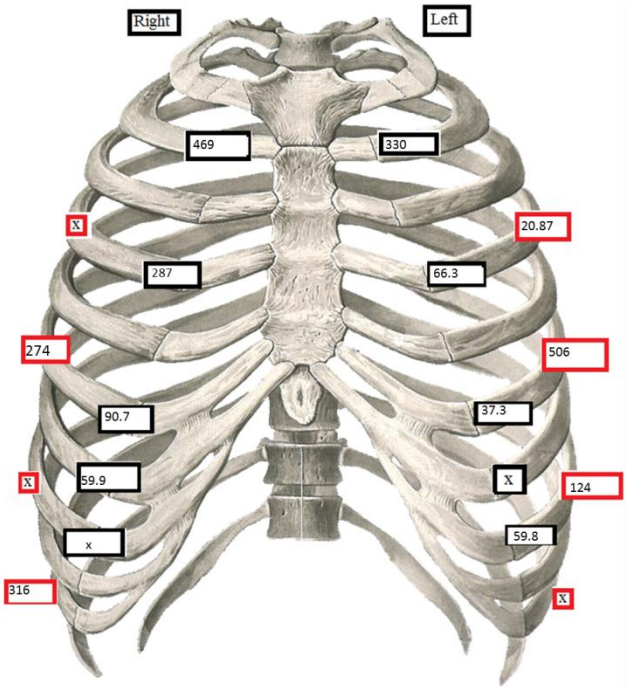

Figure 35: Test 4 and 5 anterior and middle gauge microstrain amplitudes

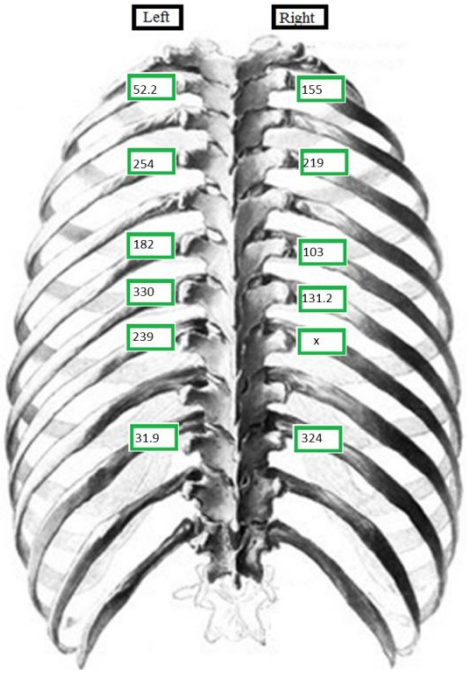

Figure 36: Test 4 and 5 posterior gauge microstrain amplitudes

Tests 4 and 5, similarly to Tests 2 and 3 without the chestband, also did not show trends across the rib surface. Figure 37 shows microstrain amplitude, inferior to superior, and by anatomical location. The right side exhibited greater strain anteriorly on ribs 2, 4, and 7 than posteriorly. Rib 2 displayed the highest average microstrain of 469 on the right side. There is no trend, either increasing or decreasing, for anterior or middle or posterior in the superior to inferior direction.

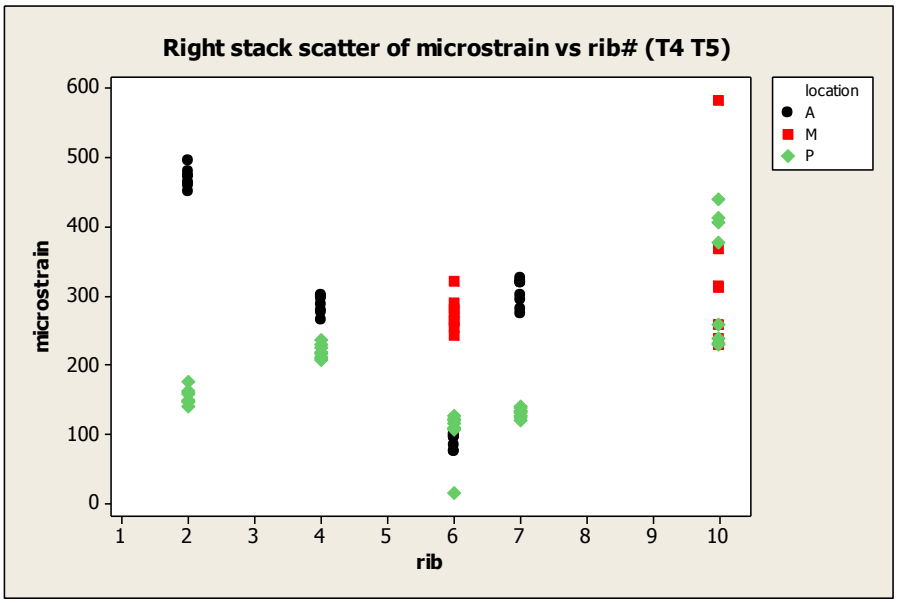

Figure 37: Right stack scatter of microstrain by rib and location (T4 T5)

Figure 38 shows microstrain amplitude inferior to superior and by anatomical location. The left side did not exhibit the same trends as the right side. Left ribs 4, 6, and 8 all display a higher average posterior strain than the anterior. This is the opposite than reported for the right side for ribs 4 and 6. Ribs 7 and 8 cannot be compared due to gauge malfunction. There is a slight trend of decreasing microstrain amplitude anteriorly in the superior to inferior direction of the rib cage on the left, but it is not as profound with the chestband on as was reported earlier with the no

chestband on the PMHS. Location L6M displayed the highest average microstrain of 506 on with the chestband on.

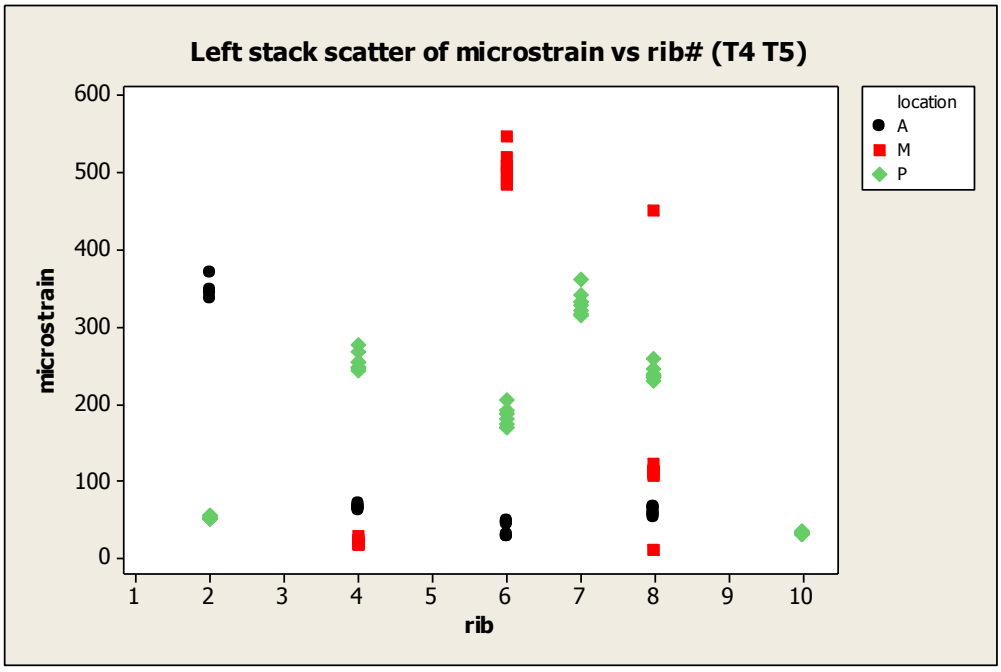

Figure 38: Left stack scatter of microstrain by rib and location (T4 T5)

Discussion

As was shown in the results section, the simulated respiration on the PHMS accurately depicted the signal produced by the *in vivo*. The ability to record deep and shallow respiration was visible in both subjects. The chestband measured the change of radial circumference of both subjects. There existed a difference in the amount of time it took for the experimental simulated breath to be created as compared to the deep inhalation in the *in vivo* subject. The simulated respiration (inhalation and exhalation) took approximately three seconds longer to produce. This manifestation difference is not thought to have any effect on the results. The time frame used to create the breath would not have as a significant impact on the strain magnitude if the depth or the volume of the breath is consistent. The PMHS took longer to obtain the set 90 cm H_2O than

the *in vivo* subject took to create a deep respiration cycle. This could mean that pressure differential created in the PMHS was larger than the pressure differential in the *in vivo* subject. The results of this increased volume would increase the strains but cannot be specifically correlated to the *in vivo* because the PMHS did not have other factors, such as muscle activation, etc.

The magnitudes of these radial changes are not identical and are not expected to be identical due to the different properties of an *in vivo subject* and PMHS. This magnitude difference can be correlated to chest circumferences, muscle interaction, and the tightness of the chestband on the subjects. The chestband was able to be considerably tighter on the PMHS since precaution was taken to ensure the comfort of the *in vivo* subject volunteer. The signals can, however, be deemed comparable, similar in shape and magnitude and only slightly stretched due to the time differences.

The strain on the bony thorax would also be altered by muscle activation during respiration. "The unitary behavior of the rib cage in normal subjects requires muscle coordination. The expansion and deflection of the bony thorax is thought to be directly related to rib rigidity and the restriction from interconnected tissue but differences in chest expansion can be seen in individuals with medical breathing complications and also in individuals during voluntary inspirations" (McCool 1985, 1703). This link was seen in the experimental setup. The *in vivo* subject was prompted to breathe deeply and naturally, making sure the chestband signals would be altered due to any "involuntary" movements caused by the forced deep breath respiration. Since the stiffness of the bony thorax is not the main factor of limiting chest expansion the muscle plays an important role in this maintaining the thorax shape (McCool 1985). Therefore it is expected that the strain levels in the PMHS should be significantly less

than would be experienced in an *in vivo subject*. The shape of the thorax is generally considered to be maintained during respiration and the interactions of the muscles should counteract the movement and deflection of the ribs caused by the lung. A pump was used to generate the PMHS breathing pattern by manually forcing air into the lungs. Doing this did not incorporate the appropriate muscle activations that are normally seen during respiration. The diaphragm initiates inhalation and this was not possible for the PMHS. The lack of muscle contractions in the internal and external intercostal muscles and the diaphragm to generate respiration is significantly different than using a respirator pump. Evaluating the microstrain produced by the expansion of the lungs will not provide a complete analysis of the strain the rib experiences but should provide a deeper understanding of the locale where higher strains are induced.

Overall, the experimental procedure displayed repeatable results. This was shown by all of the various spread plots shown in the results section. Due to lack and loss of many strain gauges, a well-defined understanding of the microstrain map across the rib (anteriorly, middle, and posteriorly) could not be established.

The expected trend of higher microstrain posteriorly than anteriorly was not shown in the data. The data showed a significant difference for anterior vs. posterior and anterior vs. middle using a Tukey-Kramer comparison test. More PMHS testing would need to be performed to confirm this result. The significance of this result can also not be seen when further broken down into analysis of the left and right sides. Also, in Tests 2 and 3, the increased microstrain occurrence at the anterior location can be attributed to the movement of the diaphragm during respiration. As the diaphragm expands, the anterior portion of the rib experiences a greater deflection with the rise of the diaphragm. This movement causes the anterior portion of the rib to move outwards. "Most of the vertical movement of the bony thorax is caused by extension

and flexion of the vertebral column, and anterior parts of the chest move more than posterior parts" (Wade 1953, 199). Therefore, the anterior portion of the rib is pressing outwards and bounded against the subcutaneous tissue. This pressure from this subcutaneous tissue resisting diaphragm expansion resulted in the higher localized microstrain on the right anterior location. This trend was not seen on the left side, though the mechanics of respiration should support this finding.

The general observation of higher posterior strain on the left side suggests that the orientation and balance of the PMHS is important. An imbalance of weight could drastically affect the rib microstrain amplitude. The vertical alignment of the PMHS via the neck brace could have unnaturally elongated the spine, pre-tensioning the posterior region of the bony thorax. Combining this with a weight imbalance, one side could be experiencing a higher strain posteriorly before respiration is even simulated. This would lead to a reduced change of microstrain because the pre-strain is masking the strain produced by the simulated respiration. Following this hypothesis, the data suggests that the left posterior side of rib cage was not 'pre-strained' to the extent of the right posterior and that the PMHS was imbalanced to the left. This orientation would pre-strain the right side prior to the simulation of respiration. Consequently, this orientation lead to decreased change of microstrain amplitude to be observed with simulated respiration on the right side. The right side pre-strain masked any change caused by the simulated respiration. Conversely, this would be opposite to what is seen on the left side. This could also lead to the inability to see symmetric loading caused by respiration on both the right and left sides of the PMHS.

Another difference that could be attributed to the differences seen in the right and left side can be highlighted by the anatomical differences between the two. It was originally thought

that the size of the lungs would not have a serious effect on the results. The resulting pressure from the lung expansion could be greater on the right than the left due to the decreased size of the left lung caused by the location of the heart inside the bony thorax.

Adding the chestband to the PMHS caused many of the microstrain readings to increase. This is expected for many of the strain gauges that are directly under the chestband, specifically towards the anterior where greater deflection occurs. This expansion will push the ribs outward while the chestband confines the expansion and rotation of the bony thorax, creating a 'pinch' interaction on the strain gauge between the rib and the chestband, creating a localized increase in strain. The volume is dispersed to other areas within the lung because the chestband confines the expansion of the chest as the pressure differential is produced. This alters the interaction between the lung expansion and the bony thorax, producing higher strains at the other locations as was consistently seen at many of the instrumented locations. For the locations that experienced a decrease in strain, the idea of the pre-strain created by the chestband may have masked the change of strain caused by the simulated inhalation, making the magnitude change appear to be less because the resting strain was increased. This result could have significant implications for the use of the chestband on other experiments. The data has shown that the chestband when added increases the strain that instrumented strain gauges experience and that it affects the gauges differently. This random increase and decrease of strain caused by the chestband could alter data leading to inaccurate conclusions. Furthermore, the chestband could result in the loss of instrumentation as was seen in testing; with many strain gauges malfunctioning after the chestband was applied and removed from the PMHS subject.

Errors and Improvements

As the results have shown, the methods used to produce the simulated respiration were repeatable and a viable comparison to the breathing pattern of an *in vivo* subject. Many other errors could contribute to the lack of trends seen in the data. The positioning of the PMHS and the lack of muscular support for the thorax could explicitly explain why no symmetry or patterns were seen. As previously mentioned, the support of the PMHS by the neck and the slightly forward posture (necessary for balance) could have created unnatural pre-existing strain on the ribs, inhibiting proper respiration posture. The magnitudes of the microstrain could be directly linked to this positioning of the PMHS. Future testing should investigate placing the PMHS in the supine position. This may increase the strain in the posterior locations but could potentially provide a more stable neutral position for comparing the strain magnitudes.

Furthermore, the lack of strain symmetry on the right and left could have been related to an unbalanced thaw of the PMHS. The temperature inside the lungs was well below normal body temperature. This temperature difference could have caused a difference in stiffness of all the responding tissue; subcutaneous, lungs, and bony thorax. This artificial increase of strength at any location could cause similar results as adding the chestband, forcing the lungs in to expand in an unconventional manner, creating increased strain at spontaneous locations. These errors could easily compound on each other, producing repeatable results that do not have any type of trends both across the rib and superior to inferior.

The lack and loss of instrumentation also did not aid in the data analysis. In order to create a better understanding of the strain caused by respiration across the rib, more gauges would be beneficial. This would help compensate for any gauges that may malfunction during testing and provide more detail along the length of the rib. Completely denuding the thorax could

also potentially improve results. Removing the subcutaneous tissue would eliminate another interactive variable and help provide an intermediate step to interpret results. A deeper investigation with more specimens may help quantify bounds and show improvements in test procedure.

Conclusion

- The methods used to simulate respiration on the PMHS subject were comparable to the *in vivo* subject.
- The data statistically supported higher strain in the anterior vs. posterior and anterior vs. middle but no significance was seen posterior vs. middle, overall the average strain decreased anterior to posterior when all the data was considered.
- Trends suggesting higher regions of strain via location, anterior, middle, and posterior were not supported when looking at individual sides (right and left)
- No trends could be seen confirming matching bilateral strain values but difference was seen between the right and left side
- No trends could be seen across the rib, by location, or superior to inferior.
- More subjects will need to be tested in order to confirm any of the proposed hypotheses
- The chestband directly altered the readings of the strain gauges fixed to the ribs and seemed to be related to the malfunction and loss of many strain gauges. Caution should be taken when analyzing strain results when the chestband has been applied to a PMHS.
- Many experimental improvements should be implemented if future testing is to occur

References

Ebacher, Vincent, Cecelia Tang, Heather McKay, Thomas R. Oxland, Pieere Guy, and Rizhi Wang. "Strain Redistribution and Cracking Behavior of Human Bone during Bending." *Bone* 40 (2007): 1265-275.

Forman, J., D. Lessley, CG. Shaw, J. Evans, R. Kent, SW. Rouhana, and P. Prasad. "Thoracic Response of Belted PMHS, the Hybrid III, and the THOR-NT Mid-Sized Male Surrogates in Low Speed, Frontal Crashes." Stapp Car Crash Journal 50 (2006): 191-215.

Gabrielli, F., D. Subit, E. Ogam, P. Guillemain, R. W. Kent, and C. Masson. "Time-frequency Analysis to Detect Bone Fracture in Impact Biomechanics. Application to the Thorax." Elsevier (2009): 952-58.

Gray, Henry. Anatomy of the Human Body. Ed. Garmine D. Clemente. 13th ed. Lea and Febiger, 1985.

Hoshaw, S. J., D. D. Cody, A. M. Saad, and D. P. Fyhrie. "Decrease in Canine Proximal Femoral Ultimate Strength and Stiffness Due to Fatigue Damage." Journal of Biomechanics 30.4 (1997): 323-29. McCool, F. Dennis, Stephen H. Loring, and Jere Mead. "Rib Cage Distortion during Voluntary and Involuntary Breathing Acts." The Journal of Applied Physiology 58.5 (1985): 1703-712.

Marieb, Elaine N. *Human Anatomy and Physiology*. 4th ed. Menlo Park, CA: Benjamin/ Cummings Science, 1998.

Russell, R.I. Ross, and P. J. Helms. "Evaluation of Three Different Techniques Used to Measure Chest Wall Movements in Children." European Respiratory Journal (1994): 2073-076.

Takahashi H; Frost HM. Age and sex related changes in the amount of cortex of normal human ribs. Acta orthopedica Scandinavia, 37: 122-30, 1966.

Verzin, P., and F. Berthet. "Structural Characterization of Human Rib Cage Behavior under Dynamic Loading." Stapp Car Crash Journal 53 (2009): 93-125.

Wade, O. L. "MOVEMENTS OF THE THORACIC CAGE AND DIAPHRAGM IN RESPIRATION." From the Pneumoconiosis Research Unit of the Medical Research Council, Cardiff (1953): 193-211.

Yoganandan N; Pintar FA. Biomechanics of human thoracic ribs. Transactions of the ASME: Journal of Biomechanical Engineering, 120: 100-4, February 1998.

Appendix A

Chestband Data Sheets

In vivo subject Chestband Orientation:

Test Number_#1: #2 :#3____
Band Number_n/a_____
Band Location_n/a_____

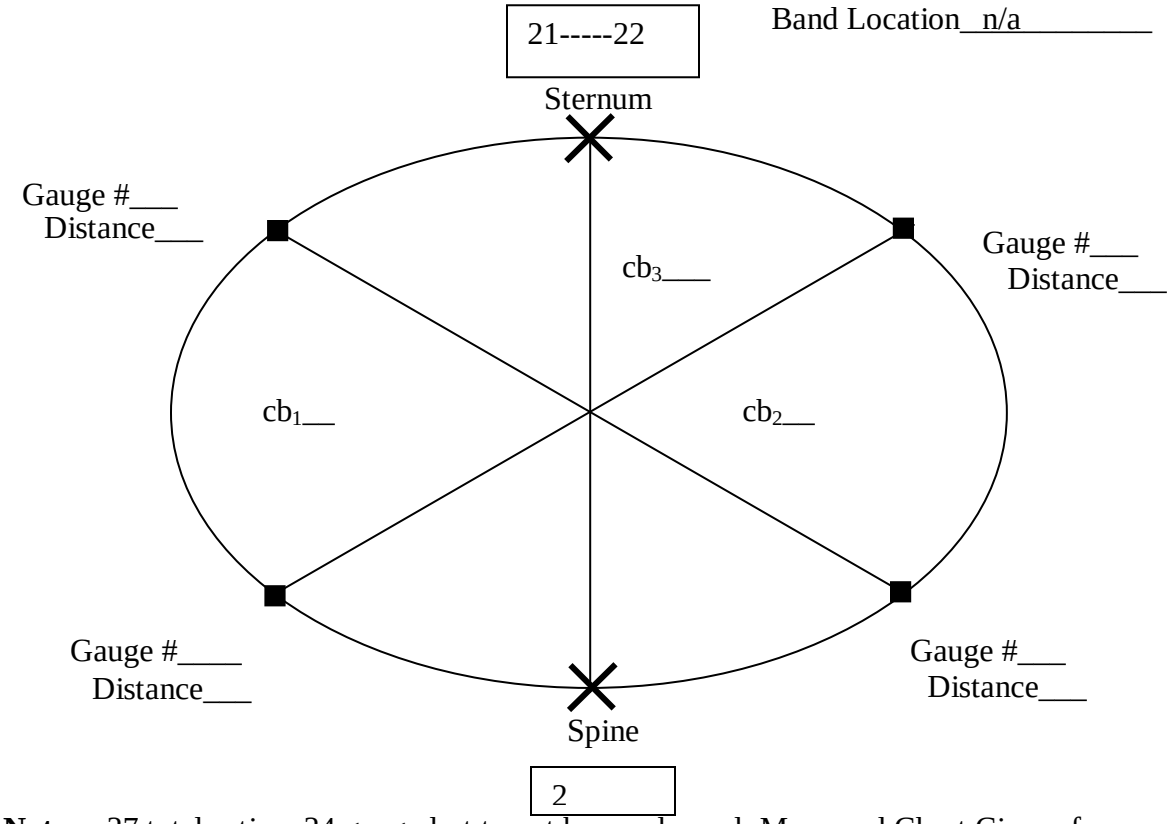

Notes: 37 total active; 34 gauge last to not be overlapped; Measured Chest Circumference =37 in

Date: 5-27-2010

In vivo subject Chestband Orientation:

*Test Number____#04; #05_*
Band Number_____
Band Location_____

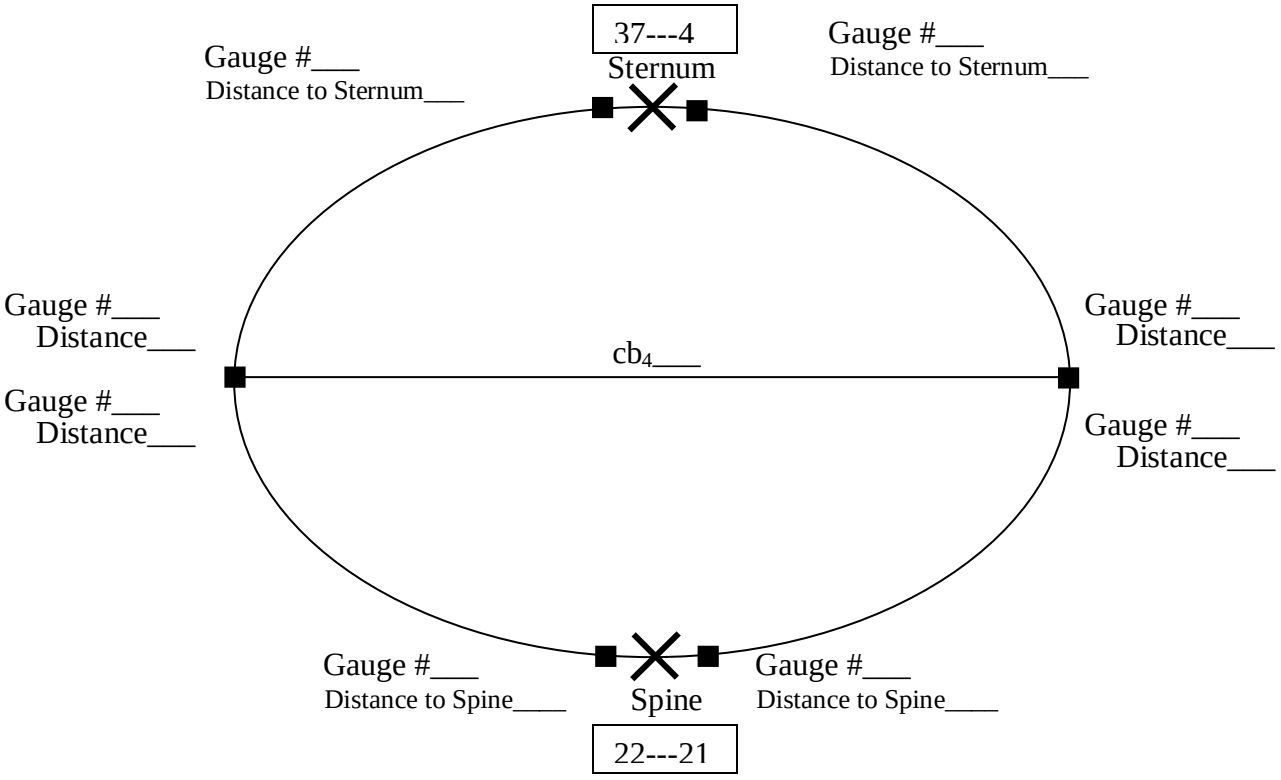

Notes: NO overlap; excess sticking out from sternum
Active gauges 4-37

In vivo subject Chestband Orientation:

Test Number____#06; #07_
Band Number_____
Band Location_____

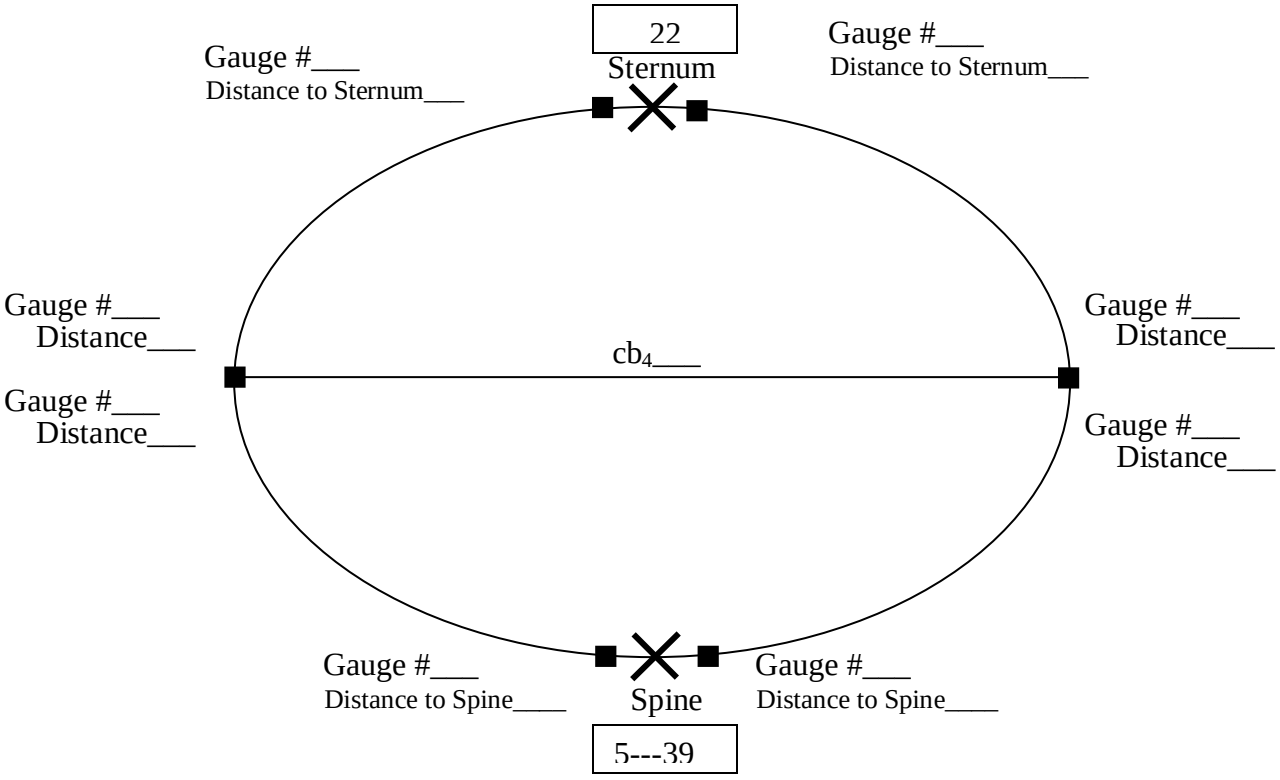

Notes: NO overlap; excess sticking out from spine
Active gauges 5-39

Date: 5-27-2010

PMHS Chestband Orientation:

Test Number____#04; #05_
Band Number_____
Band Location_____

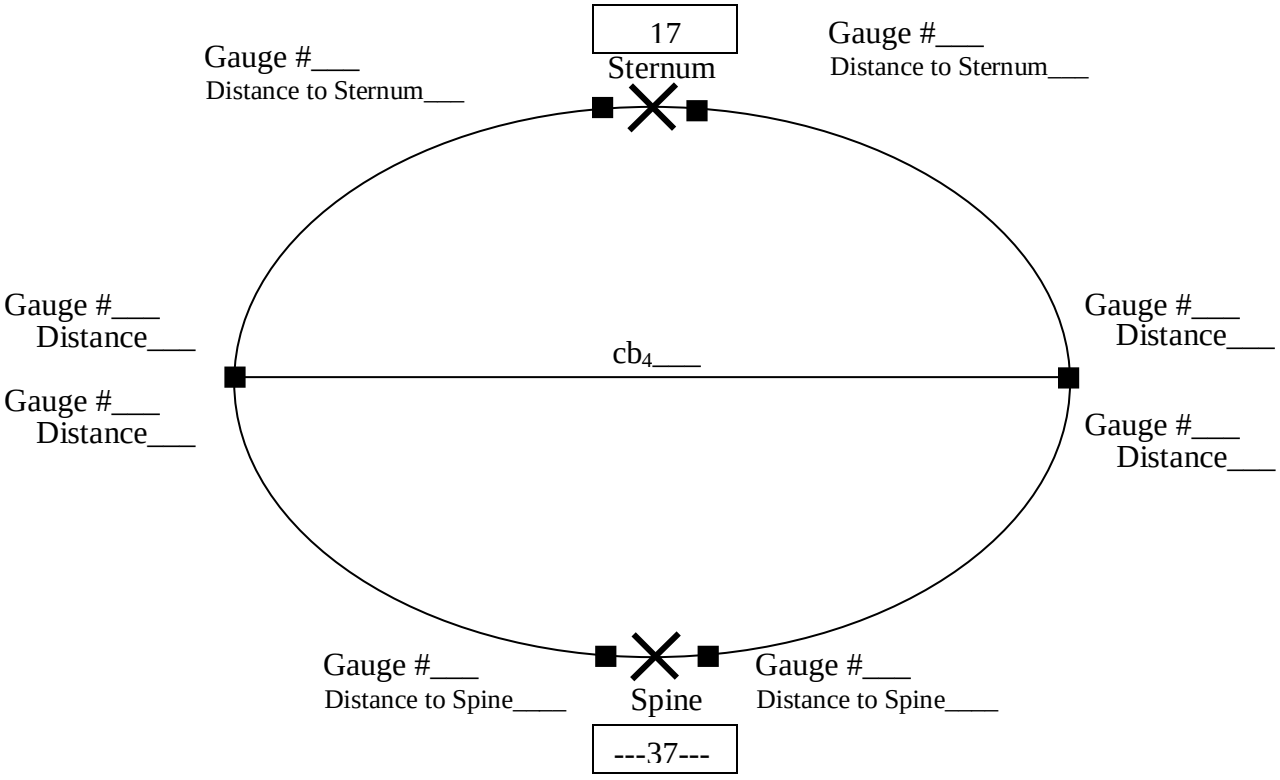

Notes: All Gauges Active, no overlap

Date: 1-10-2011

Appendix B

Anthropometric Data Sheets

Subject Data Sheet

PMHS Reference Number: ___61877_____

■ Male ☐ Female Age: _ 88____ Height: __181 cm___ Weight: ___205 lbs___ BMI: __n/a___

Cause of Death: _____
_____
_____

PMHS Appearance/Anomalies: Both subjects hips are fake, fake right knee fake as well (scars associated with all three locations), pacemaker (removed), slight scoliosis in upper thoracic lumbar verts.

Photos taken? _____n/a_____

Anthropometry Measurements (mm):

1. **STATUR** (Stature): _____1810_____
2. **SHLDHT** (Shoulder Height): _____1600_____
3. **VRTSYM** (Vertex to Symphysion Length): _____930_____
4. **SHLDBD** (Shoulder Breadth): __450_____
5. **CHSTBD** (Chest Breadth): Axillary:___305_____Xyphoid:__355_____Average:__n/a____
6. **WASTBD** (Waist Breadth): ___350_____
7. **HIPBD** (Hip Breadth): __360_____
8. **HDTROC** (Head to Trochanterion Distance): _____840_____
9. **SEATHT** (Seated Height): ____890_____
10. **INSCYE** (Interscye Distance): ___n/a_____
11. **NECKCR** (Neck Circumference): ___460_____
12. **CHSTCR** (Chest Circumference): Axillary:__1045_____Xyphoid:___1099_____Average:_n/a____
13. **WASTCR** (Waist Circumference): ____1030_____
14. **CHSTDP** (Chest Depth): Axillary:__19_____Xyphoid:____247_____Average:____n/a____
15. **WASTDP** (Waist Depth): ____182_____

Bone Mineral Density and CT Data Sheet

Pre-Test Bone Densiometry:

	Whole Body Scan	Lumbar Spine Scan
Date and Time:	**1-6-2011**	**1-6-2011**
Technician:	**Amanda Agnew**	**Amanda Agnew**
T-Score:	**1.5**	**3.7**
Notes:	**2 fake hips, fake knee**	

Pre-Test CT Scan:

	CT
Date and Time:	**1-10-2011**
Technician:	**Chad**
Session Number:	**n/a**
Notes:	**n/a**

Anterior Strain Gage Locations

Measurements taken from, 1) middle of sternum (across, A) and, 2) sternal notch (down, D)
All measurements taken in **centimeters**

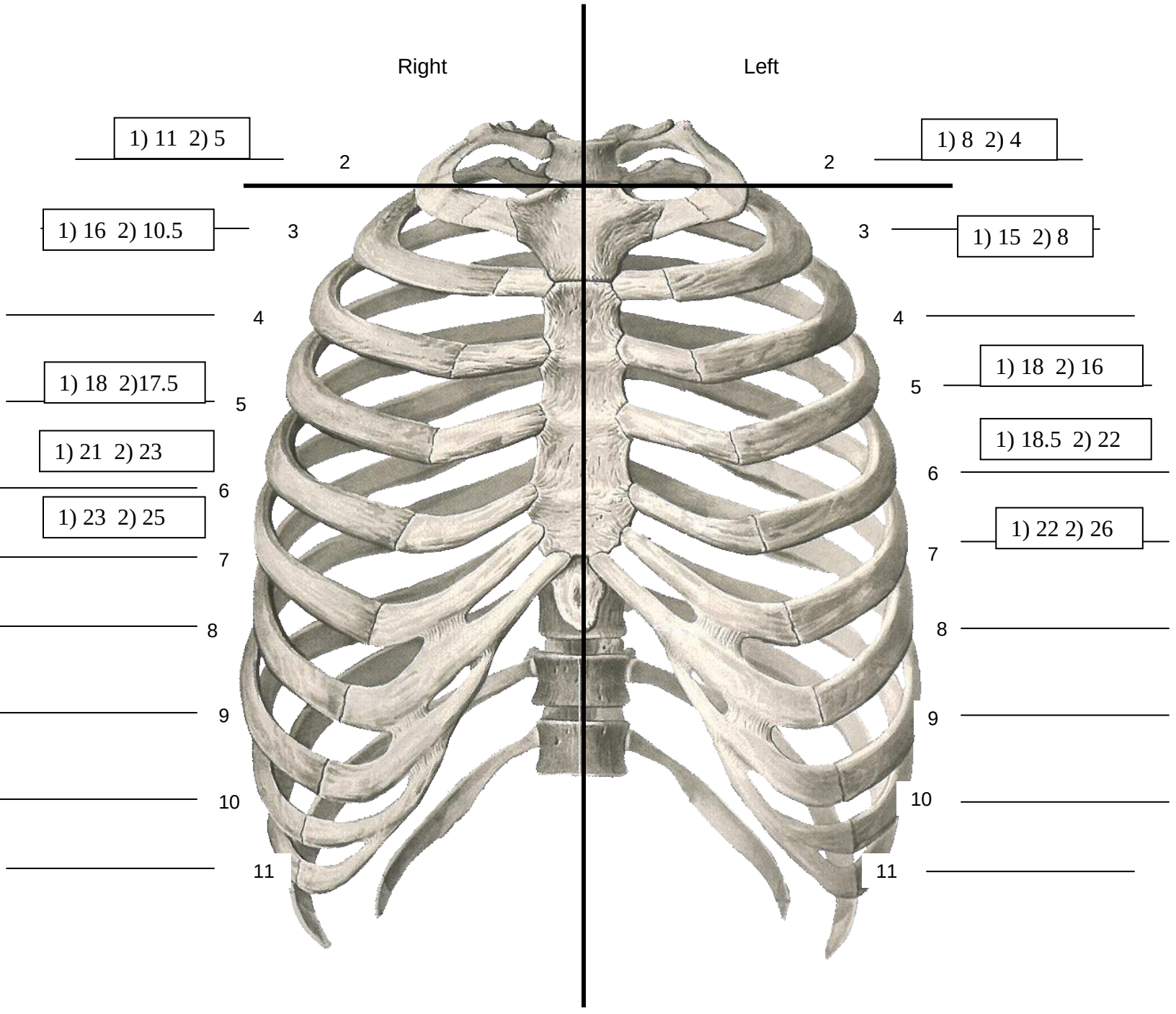

Middle Strain Gage Locations

Measurements taken from, 1) middle of sternum (across, A) and, 2) sternal notch (down, D)
All measurements taken in **centimeters**

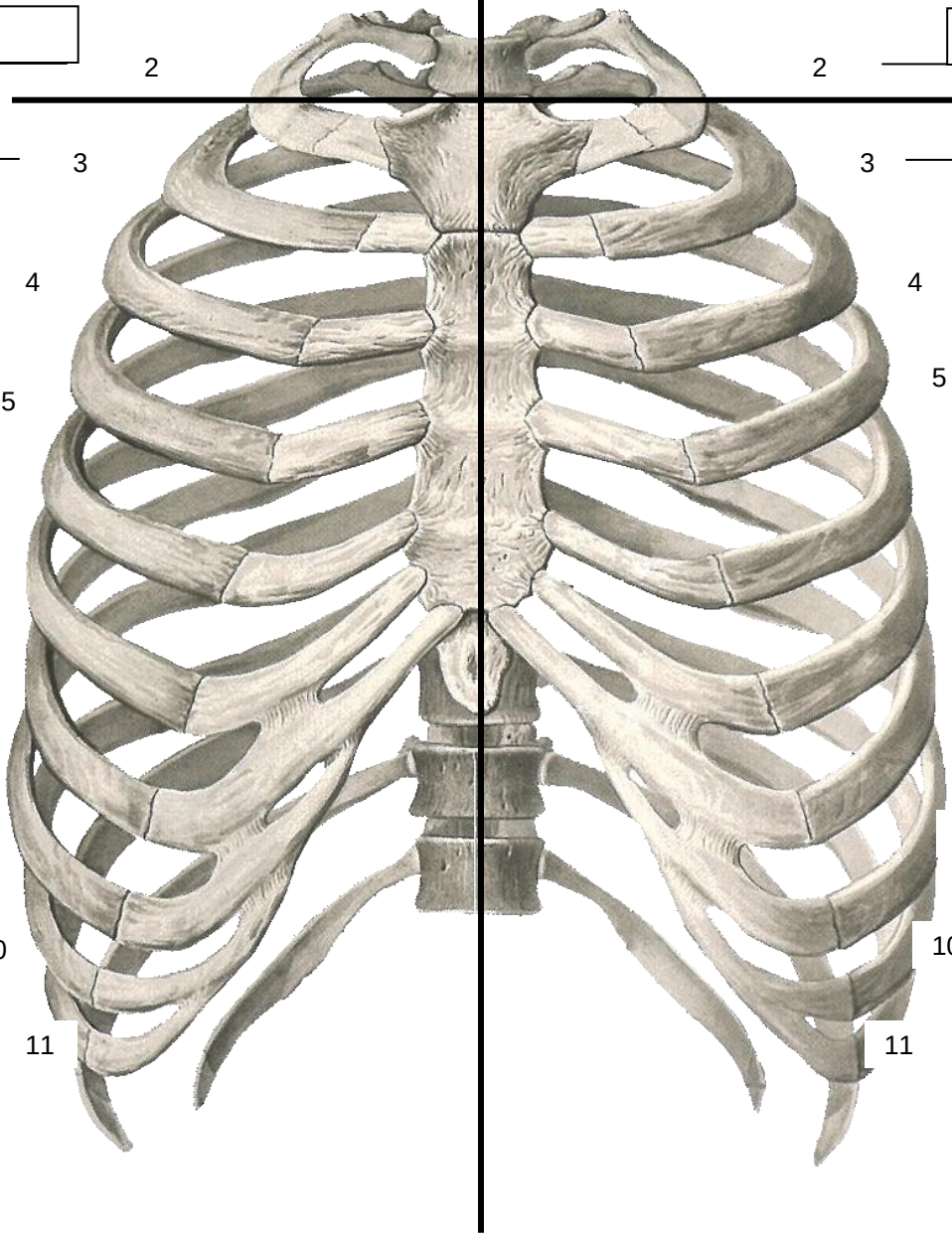

Test Data Sheet

Test Performers: __David Cagle, Amanda Agnew_____

VRTC Project Number: ___n/a_____ Test Reference Number: _____n/a_____

Test Date: _____1-11-2011_____ Test Time: __n/a_____

Test .cfg File Name: D_Cagle_PMHS_Chestbandconfig.cfg

Test Data File Name: upright_test_## Room Temperature: __74 □F Subject Temperature: __ 46□F

Data Acquisition Comments: _____n/a_____

Appendix C

MATLAB SCRIPTS

Table C 1: Chestband Data Plots , non-zeroed

```
%Chestband Data Plots
clc; close all; clear all;
data1=xlsread('Test01','Test01','A17:AO60016');
data2=xlsread('Test02','Test02','A17:AO60016');
data3=xlsread('Test03','Test03','A17:AO60016');

time1=data1(:,1);
time2=data2(:,1);
time3=data3(:,1);

%Plot with SS, no zeroing

for i=2:1:41

    figure
    plot (time1, data1(:,i),'b', time2, data2(:,i),'r', time3,
data3(:,i),'g')
    xlabel('time (sec)')
    ylabel('strain (rad/mm)')
    title(sprintf('Tests 1-3, Gauge %i',i));
    file_name=sprintf('Tests_1_thru_3_Gauge_%i.jpg',i);

    saveas(fig,file_name,'jpg')
      close all;
end
```

Table C 2: *In vivo* chestband data plots and comparisons

```
% In vivo Chestband Data Plots
clc; close all; clear all;
data1=xlsread('Test01','Test01','A17:AO60016');
time1=data1(:,1);


%Plot zero steady state
for x=1:1:40
        ave1=sum(data1(1:50,x))/length(data1(1:50,x));
        for z=1:1:length(data1)
            data1(z,x)=data1(z,x)-ave1;

        end
end

for i=17:1:17
     figure
    plot (time1, data1(:,i),'g')
    xlabel('time (sec)')
    ylabel('strain (rad/mm)')
    title(sprintf('Tests 1 Gauge %i Steady State Zeroed In Vivo ',i));
    file_name=sprintf('Tests 1 Gauge %i zeroed invivo.jpg',i);
```

```
    legend(sprintf('Chestband gauge %i',i ))
    grid on;
    saveas(gcf,file_name,'jpg')

end


%comparison of gauges that have been zeroed
%TEST 1 only

   z=22;
   for i=22:1:40
       z=z-1;
       plot (time1, data1(:,i),time1, data1(:,z))
       xlabel('time (sec)')
       ylabel('strain (rad/mm)')
       title(sprintf('Test 1 Gauge Compare %i vs %i',i,z));
       file_name=sprintf('Test_1_Gauge_Comp_%i_vs_%i.jpg',i,z);
       legend(sprintf('Run1 g%i',i), sprintf('Run1 g%i',z),'location','Best')
       grid on;
       saveas(gcf,file_name,'jpg')
   end

 %Test 3 Only

    z=22;
   for i=22:1:40
       z=z-1;
       plot (time1, data3(:,i),time1, data3(:,z))
       xlabel('time (sec)')
       ylabel('strain (rad/mm)')
       title(sprintf('Test 3 Gauge Compare %i vs %i',i,z));
       file_name=sprintf('Test_3_Gauge_Comp_%i_vs_%i.jpg',i,z);
       legend(sprintf('Run3 g%i',i), sprintf('Run3 g%i',z),'location','Best')
       grid on;
       saveas(gcf,file_name,'jpg')
   end


 %Together Test 3 and 1

 z=22;
   for i=22:1:40
       z=z-1;
       plot (time1, data3(:,i),'r',time1, data3(:,z),'b',time1, data1(:,i),'-
-r',time1, data1(:,z),'--b')
       xlabel('time (sec)')
       ylabel('strain (rad/mm)')
       title(sprintf('Tests 1 and 3 Gauge Compare %i vs %i',i,z));
       file_name=sprintf('Test_1_and_3_Gauge_Comp_%i_vs_%i.jpg',i,z);
       legend(sprintf('Run3 g%i',i), sprintf('Run3 g%i',z),sprintf('Run1
g%i',i),sprintf('Run1 g%i',z),'location','Best')
```

```
        grid on;
        saveas(gcf,file_name,'jpg')
    end
```

Table C 3: PMHS Chestband data analysis plots

```
% PMHS chestband data analysis plots

clear all; close all; clc;

for b=4:1:4
    fileopen=sprintf('upright_test_0%i.txt',b);
    data=importdata(fileopen);
    time=data(:,1);
    size(data);
    data=data(:,33:72);
    sens=[343.4 353.4 251.4 274.8 299.8 339.8 293.4 339.8 345.8 200 272.2
330.6 253.4 357 339.4 337.4 326.6 333.8 314.8 316.4 327.4 319.8 317 316.2
329.4 287.8 328 331.2 325 330.4 316.6 317.8 320.4 328 318.8 314.4 313 311.6
302.6 353.4];
    for zeta=1:1:length(sens)
        for beta=1:1:length(data)
            data(beta,zeta)=data(beta,zeta)*.2/sens(zeta); % convert to right
units rad/mm
        end
    end
    for x=1:1:40
        ave1=sum(data(1:50,x))/length(data(1:50,x));
        for z=1:1:length(data)
            data(z,x)=data(z,x)-ave1;

        end
    end

    for i=1:1:40
        figure
        plot (time, data(:,i),'b')
        xlabel('time (sec)')
        ylabel('strain (rad/mm)')
        title(sprintf('Test 4 Gauge %i Steady State Zeroed PMHS',i));
        file_name=sprintf('Test 4 Gauge_%i_zeroed_PMHS.jpg',i);
        legend(sprintf('Chestband gauge %i',i))
        grid on;
        saveas(gcf,file_name,'jpg')

    end
end
```

Table C 4: Show only y-values on data point labels

```
function output_txt =showyonly(obj,event_obj)
% Display the position of the data cursor
% obj          Currently not used (empty)
% event_obj    Handle to event object
% output_txt   Data cursor text string (string or cell array of strings).

pos = get(event_obj,'Position');
output_txt = {['Y: ',num2str(pos(2),4)]};
%['X: ',num2str(pos(1),4)],...
% If there is a Z-coordinate in the position, display it as well
if length(pos) > 2
    output_txt{end+1} = ['Z: ',num2str(pos(3),4)];
end
```

Table C 5: Show only x-values on data point labels

```
function output_txt = showxonly(obj,event_obj)
% Display the position of the data cursor
% obj          Currently not used (empty)
% event_obj    Handle to event object
% output_txt   Data cursor text string (string or cell array of strings).

pos = get(event_obj,'Position');
output_txt = {['X: ',num2str(pos(1),4)]};

% If there is a Z-coordinate in the position, display it as well
if length(pos) > 2
    output_txt{end+1} = ['Z: ',num2str(pos(3),4)];
end
```

Table C 6: Import Text File Data

```
function importfile(fileToRead1)
%IMPORTFILE(FILETOREAD1)
%  Imports data from the specified file
%  FILETOREAD1:  file to read

%  Auto-generated by MATLAB on 20-Jan-2011 17:25:19

% Import the file
rawData1 = importdata(fileToRead1);

% For some simple files (such as a CSV or JPEG files), IMPORTDATA might
% return a simple array.  If so, generate a structure so that the output
% matches that from the Import Wizard.
[unused,name] = fileparts(fileToRead1);
newData1.(genvarname(name)) = rawData1;
```

```
 % Create new variables in the base workspace from those fields.
vars = fieldnames(newData1);
for i = 1:length(vars)
    assignin('base', vars{i}, newData1.(vars{i}));
end
```

Table C 7: PMHS Strain Gauge Analysis- Peak Analysis

```
%Strain Gauge data analysis

clear all; close all; clc;

for b=2:1:2
    fileopen=sprintf('upright_test_0%i.txt',b);
    data=importdata(fileopen);
    time=data(:,1);
    size(data);

    for x=3:1:32
        ave1=sum(data(1:50,x))/length(data(1:50,x));
        for z=1:1:60000
            data(z,x)=data(z,x)-ave1;

        end
    end
    name_gauge= ['L8M ' 'L2A ' 'L2P ' 'L4A ' 'L4M ' 'L4P ' 'L6A ' 'L6M ' 'L6P
' 'L7A ' 'L7P ' 'L8A ' 'L8P ' 'L10M' 'L10P' 'R2A ' 'R2P ' 'R4A ' 'R4M ' 'R4P
' 'R6A ' 'R6M ' 'R6P ' 'R7A ' 'R7P ' 'R8A ' 'R8M ' 'R8P ' 'R10M' 'R10P'];
    y=2;
    location=2;
    for i=3:1:4
        [peaks,mags]=peakfinder(data(:,i),15,1);
        [peaks2,mags2]=peakfinder(data(:,i),15,-1);
        peakfinder(data(:,i),15,1);
        xlabel('time (seconds)')
        ylabel('micro-strain (dimensionless)')
        filename=sprintf('%s%s%s%s Test_%i max pts',name_gauge(y-
1),name_gauge(y+0),name_gauge(y+1),name_gauge(y+2),b);
        titlename= sprintf('%s%s%s%s Strain Response Test %i
maxpts',name_gauge(y-1),name_gauge(y+0),name_gauge(y+1),name_gauge(y+2),b);
        title(titlename)
        saveas(gcf,filename,'fig')
        close all;
         peakfinder(data(:,i),15,-1);
        xlabel('time (seconds)')
        ylabel('micro-strain (dimensionless)')
        filename=sprintf('%s%s%s%s Test_%i min pts',name_gauge(y-
1),name_gauge(y+0),name_gauge(y+1),name_gauge(y+2),b);
        titlename= sprintf('%s%s%s%s Strain Response Test %i
minpts',name_gauge(y-1),name_gauge(y+0),name_gauge(y+1),name_gauge(y+2),b);
        title(titlename)
        saveas(gcf,filename,'fig')
```

```
        y=y+4;
        close all
    end

    clear data
    clear time
end
```

Table C 8: PMHS Data analysis comparison via location

```
%data analysis PMHS

clear all; close all; clc;

for b=2:1:8
    fileopen=sprintf('upright_test_0%i.txt',b);
    data=importdata(fileopen);
    time=data(:,1);
    size(data);

    for x=3:1:32
        ave1=sum(data(1:50,x))/length(data(1:50,x));
        for z=1:1:60000
            data(z,x)=data(z,x)-ave1;

        end
    end


    name_gauge= ['L2A ' 'L2P ' 'L4A ' 'L4M ' 'L4P ' 'L6A ' 'L6M ' 'L6P ' 'L7A
' 'L7P ' 'L8A ' 'L8M '  'L8P ' 'L10M' 'L10P' 'R2A ' 'R2P ' 'R4A ' 'R4M ' 'R4P
' 'R6A ' 'R6M ' 'R6P ' 'R7A ' 'R7P ' 'R8A ' 'R8M ' 'R8P ' 'R10M' 'R10P'];
    name_gauge2= ['R2A ' 'R2P ' 'R4A ' 'R4M ' 'R4P ' 'R6A ' 'R6M ' 'R6P '
'R7A ' 'R7P ' 'R8A ' 'R8M ' 'R8P ' 'R10M' 'R10P'];

    y=2;
    high=18;
    for i=4:1:14

        figure
        plot(time, data(:,i),time, data(:,high))
        xlabel('time (seconds)')
        ylabel('micro-strain (dimensionless)')

        filename=sprintf('%s%s%s%s vs %s%s%s%s Strain Response Test
%i',name_gauge(y-
1),name_gauge(y+0),name_gauge(y+1),name_gauge(y+2),name_gauge2(y-
1),name_gauge2(y+0),name_gauge2(y+1),name_gauge2(y+2),b);
        titlename= sprintf('%s%s%s%s vs %s%s%s%s Strain Response Test
%i',name_gauge(y-
```

```
1),name_gauge(y+0),name_gauge(y+1),name_gauge(y+2),name_gauge2(y-
1),name_gauge2(y+0),name_gauge2(y+1),name_gauge2(y+2),b);
        title(titlename)
        legend(sprintf('%s%s%s%s',name_gauge(y-
1),name_gauge(y+0),name_gauge(y+1),name_gauge(y+2)),sprintf('%s%s%s%s',name_g
auge2(y-
1),name_gauge2(y+0),name_gauge2(y+1),name_gauge2(y+2)),'location','Best');
        saveas(gcf,filename,'jpg')
        y=y+4;
        close all
       high=high+1;
    end
    y=y+4;
    high=30;
    for i=15:1:17

        figure
        plot(time, data(:,i),time, data(:,high))
        xlabel('time (seconds)')
        ylabel('micro-strain (dimensionless)')

        filename=sprintf('%s%s%s%s vs %s%s%s%s Strain Response Test
%i',name_gauge(y-
1),name_gauge(y+0),name_gauge(y+1),name_gauge(y+2),name_gauge2(y-
1),name_gauge2(y+0),name_gauge2(y+1),name_gauge2(y+2),b);
        titlename= sprintf('%s%s%s%s vs %s%s%s%s Strain Response Test
%i',name_gauge(y-
1),name_gauge(y+0),name_gauge(y+1),name_gauge(y+2),name_gauge2(y-
1),name_gauge2(y+0),name_gauge2(y+1),name_gauge2(y+2),b);
        title(titlename)
        legend(sprintf('%s%s%s%s',name_gauge(y-
1),name_gauge(y+0),name_gauge(y+1),name_gauge(y+2)),sprintf('%s%s%s%s',name_g
auge2(y-
1),name_gauge2(y+0),name_gauge2(y+1),name_gauge2(y+2)),'location','Best');
        saveas(gcf,filename,'jpg')
        y=y+4;
        close all
       high=high+1;
    end

    figure
    plot(time, data(:,3),time, data(:,28))
    xlabel('time (seconds)')
    ylabel('micro-strain (dimensionless)')
    filename=sprintf('L8M vs R8M Strain Response Test %i',b);
    titlename= sprintf('L8M vs R8M Strain Response Test %i',b);
    title(titlename)
    legend('L8M','R8M','location','Best')
    saveas(gcf,filename,'jpg')
    clear data
    clear time
end
```

Table C 9: Peak Finder Function

```
function varargout = peakfinder(x0, thresh, extrema)
%PEAKFINDER Noise tolerant fast peak finding algorithm
%   INPUTS:
%       x0 - A real vector from the maxima will be found (required)
%       thresh - The amount above surrounding data for a peak to be
%           identified (default = (max(x0)-min(x0))/4). Larger values mean
%           the algorithm is more selective in finding peaks.
%       extrema - 1 if maxima are desired, -1 if minima are desired
%           (default = maxima, 1)
%   OUTPUTS:
%       peakLoc - The indicies of the identified peaks in x0
%       peakMag - The magnitude of the identified peaks
%
%   [peakLoc] = peakfinder(x0) returns the indicies of local maxima that
%       are at least 1/4 the range of the data above surrounding data.
%
%   [peakLoc] = peakfinder(x0,thresh) returns the indicies of local maxima
%       that are at least thresh above surrounding data.
%
%   [peakLoc] = peakfinder(x0,thresh,extrema) returns the maxima of the
%       data if extrema > 0 and the minima of the data if extrema < 0
%
%   [peakLoc, peakMag] = peakfinder(x0,...) returns the indicies of the
%       local maxima as well as the magnitudes of those maxima
%
%   If called with no output the identified maxima will be plotted along
%       with the input data.
%
%   Note: If repeated values are found the first is identified as the peak
%
% Ex:
% t = 0:.0001:10;
% x = 12*sin(10*2*pi*t)-3*sin(.1*2*pi*t)+randn(1,numel(t));
% x(1250:1255) = max(x);
% peakfinder(x)
%
% Copyright Nathanael C. Yoder 2009 (ncyoder@purdue.edu)

% Perform error checking and set defaults if not passed in
error(nargchk(1,3,nargin,'struct'));
error(nargoutchk(0,2,nargout,'struct'));

s = size(x0);
flipData =  s(1) < s(2);
len0 = numel(x0);
if len0 ~= s(1) && len0 ~= s(2)
    error('PEAKFINDER:Input','The input data must be a vector')
elseif isempty(x0)
```

```
    varargout = {[],[]};
    return;
end
if ~isreal(x0)
    warning('PEAKFINDER:NotReal','Absolute value of data will be used')
    x0 = abs(x0);
end

if nargin < 2 || isempty(thresh)
    thresh = (max(x0)-min(x0))/4;
elseif ~isnumeric(thresh) || ~isreal(thresh)
    thresh = (max(x0)-min(x0))/4;
    warning('PEAKFINDER:VectorThresh',...
        sprintf('The threshold must be a real scalar.  A threshold of %.4g
will be used',thresh))
elseif numel(thresh) > 1
    warning('PEAKFINDER:VectorThresh','The threshold must be a scalar.  The
first threshold in the vector will be used.')
    thresh = thresh(1);
end
if nargin < 3 || isempty(extrema)
    extrema = 1;
else
    extrema = sign(extrema(1)); % Should only be 1 or -1 but make sure
    if extrema == 0
        error('PEAKFINDER:ZeroMaxima','Either 1 (for maxima) or -1 (for
minima) must be input for extrema');
    end
end

x0 = extrema*x0(:); % Make it so we are finding maxima regardless
dx0 = diff(x0); % Find derivative
dx0(dx0 == 0) = -eps; % This is so we find the first of repeated values
ind = find(dx0(1:end-1).*dx0(2:end) < 0)+1; % Find where the derivative
changes sign

% Include endpoints in potential peaks and valleys
x = [x0(1);x0(ind);x0(end)];
ind = [1;ind;len0];

% x only has the peaks, valleys, and endpoints
len = numel(x);
minMag = min(x);


if len > 2 % Function with peaks and valleys

    % Set initial parameters for loop
    tempMag = minMag;
    foundPeak = false;
    leftMin = minMag;
```

```
    % Deal with first point a little differently since tacked it on
    % Calculate the sign of the derivative since we taked the first point
    %  on it does not neccessarily alternate like the rest.
    signDx = sign(diff(x(1:3)));
    if signDx(1) <= 0 % The first point is larger or equal to the second
        ii = 0;
        if signDx(1) == signDx(2) % Want alternating signs
            x(2) = [];
            ind(2) = [];
            len = len-1;
        end
    else % First point is smaller than the second
        ii = 1;
        if signDx(1) == signDx(2) % Want alternating signs
            x(1) = [];
            ind(1) = [];
            len = len-1;
        end
    end

    % Preallocate max number of maxima
    maxPeaks = ceil(len/2);
    peakLoc = zeros(maxPeaks,1);
    peakMag = zeros(maxPeaks,1);
    cInd = 1;
    % Loop through extrema which should be peaks and then valleys
    while ii < len
        ii = ii+1; % This is a peak
        % Reset peak finding if we had a peak and the next peak is bigger
        %   than the last or the left min was small enough to reset.
        if foundPeak && (x(ii) > peakMag(end) || leftMin < peakMag(end)-
thresh)
            tempMag = minMag;
            foundPeak = false;
        end

        % Make sure we don't iterate past the length of our vector
        if ii == len
            break; % We assign the last point differently out of the loop
        end

        % Found new peak that was larger than temp mag and threshold larger
        %   than the minimum to its left.
        if x(ii) > tempMag && x(ii) > leftMin + thresh
            tempLoc = ii;
            tempMag = x(ii);
        end

        ii = ii+1; % Move onto the valley
        % Come down at least thresh from peak
        if ~foundPeak && tempMag > thresh + x(ii)
            foundPeak = true; % We have found a peak
```

```
            leftMin = x(ii);
            peakLoc(cInd) = tempLoc; % Add peak to index
            peakMag(cInd) = tempMag;
            cInd = cInd+1;
        elseif x(ii) < leftMin % New left minima
            leftMin = x(ii);
        end
    end

    % Check end point
    if x(end) > tempMag && x(end) > leftMin + thresh
        peakLoc(cInd) = len;
        peakMag(cInd) = x(end);
        cInd = cInd + 1;
    elseif ~foundPeak && tempMag > minMag % Check if we still need to add the
last point
        peakLoc(cInd) = tempLoc;
        peakMag(cInd) = tempMag;
        cInd = cInd + 1;
    end

    % Create output
    peakInds = ind(peakLoc(1:cInd-1));
    peakMags = peakMag(1:cInd-1);
else % This is a monotone function where an endpoint is the only peak
    [peakMags,xInd] = max(x);
    if peakMags > minMag + thresh
        peakInds = ind(xInd);
    else
        peakMags = [];
        peakInds = [];
    end
end
 % Rotate data if needed
if flipData
    peakMags = peakMags.';
    peakInds = peakInds.';
end
% Change sign of data if was finding minima
if extrema < 0
    peakMags = -peakMags;
    x0 = -x0;
end
% Plot if no output desired
if nargout == 0
    if isempty(peakInds)
        disp('No significant peaks found')
    else
        figure;
        plot(1:len0,x0,'.-',peakInds,peakMags,'ro','linewidth',2);
    end
else
    varargout = {peakInds,peakMags};
```

```
end
```